University of Helsinki
Faculty of Science
Department of Chemistry
Finland

Assessing toxicity of ionic liquids utilizing zebrafish, cells, and liposomes

Suvi-Katriina Ruokonen

ACADEMIC DESSERTATION

To be presented, with the permission of the Faculty of Science of the University of Helsinki,
for public criticism in Auditorium A110 of the Department of Chemistry
on October 12th, 2018, at 12 o'clock
Helsinki 2018

Supervisor: Docent Susanne Wiedmer
Department of Chemistry
University of Helsinki
Finland

Reviewers: Professor João Coutinho
Department of Chemistry
University of Aveiro
Portugal

Associate Professor Christian Jungnickel
Faculty of Chemistry
Gdańsk University of Technology
Poland

Opponent: Professor Jonas Berqvist
Department of Chemistry
University of Uppsala
Sweden

ISBN 978-951-51-4413-3 (paperback)
ISBN 978-951-51-4414-0 (pdf)

http://ethesis.helsinki.fi
Unigrafia, Helsinki 2018

ABSTRACT

Ionic liquids are molten salts, with melting points usually below 100 °C. Because the physical and chemical properties of ionic liquids are easily tunable by combining different ionic liquid cations and anions, has their use become more popular in many pharmaceutical and industrial applications. Despite their “green reputation”, due to their low vapor pressures and growing use, there is only little information on the toxicity of ionic liquids, effects on the environment, and long-term impacts. Many ionic liquids are water-soluble and lipophilic, thus they can bioaccumulate in aqueous organisms and furthermore in animals at higher trophic levels and eventually even to humans.

This doctoral thesis describes how a group of phosphonium-, imidazolium-, and guanidinium-based ionic liquids interact with zebrafish, various cell lines, and biomimicking phospholipid vesicles (liposomes). The ionic liquids in this study are potential biomass dissolvers. Further, the ionic liquids were chosen to have different chain lengths or core atoms. The aim of the study was to determine how the selection of a target organism, cation chain length, and especially anion chain length of phosphonium-based ionic liquids affect the ionic liquid toxicity. In addition, a long-term exposure to potential biomass dissolving ionic liquids was assessed using adult zebrafish. These results were utilized to find novel methodologies to evaluate ionic liquid toxicity without the use of living organisms, using solely cell membrane mimicking liposomes. To investigate the influence of ionic liquids on cell rupturing, hemolysis and a real-time cytotoxicity assay were performed and the results were compared with liposome integrity information. Differential scanning calorimetry was used to study the penetration of the ionic liquid into the lipid bilayer. The effect of ionic liquids on the size and the zeta potential of negatively charged liposomes, were assessed in order to obtain information on the changes in the diameter and surface charge of the liposomes. In addition, nuclear magnetic resonance spectroscopy, more specifically diffusion ordered spectroscopy was utilized for studying whether the ionic liquids occur as unimers or aggregates and if they are attached to the lipid bilayer.

By comparing the toxicity results obtained from the zebrafish and cytotoxicity assays to the lipid bilayer rupturing information, it was possible to predict the mechanism of toxicity of ionic liquids. Thus, the ionic liquids could be divided into three groups based on their toxicity mechanism: 1) plasma membrane rupturing ionic liquids, 2) ionic liquids that have an effect on both the cell membrane integrity and the cell metabolism, and 3) ionic liquids affecting solely on the cell metabolism.

PREFACE

This thesis research was carried out at the Department of Chemistry at the University of Helsinki during the years 2014–2018. I thank the heads of the Department Prof. Markku Räsänen and Prof. Heikki Tenhu for the opportunity to conduct my research here and providing the research facilities. The Academy of Finland and CHEMS-doctoral program are greatly acknowledge for the financial support of this thesis.

First, I wish to express my deepest gratitude to my supervisor Docent Susanne Wiedmer. It has been a privilege to work under the supervision of an efficient and inspirational scientist like her. Susanne has always had her door open for me regarding scientific discussions but also regarding life itself. I can only thank her for all the things I have learnt during these past four years and for giving me the freedom of fulfilling myself despite of my stubborn nature. In addition of being an excellent supervisor I am also glad to been able to share my free-time and hobbies with her.

Next, I want to thank the reviewers Professor João Coutinho and Associate Professor Christian Jungnickel of this thesis for putting their time to delve into my thesis and giving their valuable comments.

I am grateful for been able to collaborate with such many talented scientists. I would like to acknowledge Prof. Ilkka Kilpeläinen and Docent Alistair King for their input on planning and supervising the synthesis of all the ionic liquids used in this work. Also, I would like to express my gratitude to their group members, MSc Kashmira Vyavakar, PhD Ashley Holding, PhD Arno Parviainen, and PhD Evangelos Sklavounos for providing the samples.

I would like to thank Prof. Michael Lämmerhofer and his group members, MSc Corinna Sanwald and PhD Stefan Polnick, for the opportunity to conduct experiments at the University of Tübingen, Germany and their help and assistance. I would also like to thank Prof. Pertti Panula and PhD Maria Sundvik, for the opportunity to perform toxicity studies on zebrafish at the Anatomy Department, University of Helsinki, and for sharing their knowledge and assistance. The late Prof. Juha Holopainen and PhD Alexandra Robciuc, from the Department of Ophthalmology, University of Helsinki, Helsinki University Hospital, are greatly acknowledged for their excellent collaboration in many mutual projects. Phil.Lic. Matti Jussila and Karina Moslova are much thanked for their technical assistance and for keeping the instruments running. I also want to thank Docent Sami Hietala for his technical and scientific help with the liposome studies. I owe my gratitude also to Prof. Dage Sundholm and the former Swedish laboratory group, who made the working environment excellent from the beginning of my research path.

I have been privileged to have been able to work and learn from amazing post-docs. First, I would like to show my gratitude to PhD Jana Lokajová, PhD Ján Petrovaj, and PhD Inkeri Kontro with whom I have had the privilege to work with. Next, I would like to thank PhD Filip Duša for his endless help with capillary electrophoresis measurements and fruitful discussions, PhD Wen Chen for her always-positive attitude, and Docent Filip Ekholm for many discussions of science and life and his optimistic sense of humor. Finally, I want to express my sincerest appreciation to PGs PhD Joanna Witos and PhD Antti Rantamäki for the awesome atmosphere that they have created in our group, the countless brainstorming sessions, sharing my sense of humor, and for their friendship.

Finally, I would like to thank my awesome friends. You have offered me a well-needed time-off from work. Thank you also for your support and for the patience listening of “work stuff nobody understands”.

My parents Ritva and Markku and my siblings Tuuli and Jouko are greatly acknowledged for their never-ending love and support and for making me the person I am today.

Above all, I want to thank my husband Roope for his patience, understanding, and support. Thank you for making me laugh when I have needed it. You made this process much easier.

Helsinki, 30.06.2018

CONTENTS

LIST OF ORIGINAL PUBLICATIONS

The doctoral dissertation is based on the following publications, hereafter referred to by their Roman numerals [I–V]:

I. **Ruokonen, S.-K**.; Sanwald, C.; Sundvik, M.; Polnick, S.; Vyavaharkar, K.; Duša, F.; Holding, A.J.; King, A.W.T.; Kilpeläinen, I.; Lämmerhofer, M.; Panula, P.; Wiedmer, S.K., Effect of ionic liquids on zebrafish (*Danio rerio*) viability, behavior, and histology; correlation between toxicity and ionic liquid aggregation. *Environmental Science and Technology,* 2016, 50, (13), 7116–7125.

II. **Mikkola, S.-K**.*; Robciuc, A.; Lokajová, J.; Holding, A.J.; Lämmerhofer, M.; Kilpeläinen, I.; Holopainen, J.M.; King, A.W.T.; Wiedmer, S.K., Impact of amphiphilic biomass-dissolving ionic liquids on biological cells and liposomes. *Environmental Science and Technology,* 2015, 49, (3), 1870–1878. (* Ruokonen, *neé* Mikkola).

III. **Ruokonen, S.-K**.; Duša, F.; Rantamäki, A.H.; Robciuc, A.; Holma, P.; Holopainen, J.M.; Abdel-Rehim, M.; Wiedmer, S.K., Distribution constants of local anesthetics between aqueous and liposome phases. *Journal of Chromatography A,* 2017, 1479, 194–203.

IV. Rantamäki A.H.; **Ruokonen S.-K**.; Sklavounos E.; Kyllönen, L.; King A.W.T.; Wiedmer S.K., Impact of surface-active guanidinium-, tetramethylguanidinium- and cholinium-based ionic liquids on *Vibrio fischeri* cells and dipalmitoylphophatidylcholine liposomes. *Scientific Reports,* 2017, 7, 1–12.

V. **Ruokonen, S.-K**.; Sanwald, C.; Robciuc, A.; Hietala, S.; Rantamäki, A.H.; Witos, J.; King, A.W.T.; Lämmerhofer, M.; Wiedmer, S.K., Correlation between ionic liquid toxicity and liposome-ionic liquid interactions. *Chemistry – A European Journal,* 2018, 24, (11), 2669–2680.

Contribution of the author:

Experimental work related to fish studies (paper I), preliminary cell studies (paper I), and cytotoxicity assay of *Escherichia coli* bacteria (paper II), as well as critical micelle concentration (papers I–III), capillary electrophoresis (paper II), liposome electrokinetic chromatography (paper III), and liposome studies including dynamic light scattering (paper II, V), zeta potential (paper II, V), differential scanning calorimetry (paper IV, V), and nuclear magnetic resonance spectroscopy (paper V) determinations. Preliminary experimental work (paper IV) and assistance with the *Vibrio fischeri*

cytotoxicity assays (paper V). Data analysis of all results (papers I–V) and main responsibility of writing the manuscripts (papers I–III and V). Assistance and reviewing of paper IV.

Publications not included in the thesis:

Ruokonen, S.-K.; Duša, F.; Lokajová, J.; Kilpeläinen, I.; King, A.W.T.; Wiedmer, S.K., Effect of ionic liquids on the interaction between liposomes and common wastewater pollutants investigated by capillary electrophoresis. *Journal of Chromatography A,* 2015, 1405, 178–187.

Duša, F.; **Ruokonen, S.-K**.; Petrovaj, J.; Viitala, T.; Wiedmer, S. K., Ionic liquids affect the adsorption of liposomes onto cationic polyelectrolyte coated silica evidenced by quartz crystal microbalance. *Colloids and Surfaces B: Biointerfaces,* 2015, 136, 496–505.

Kontro, I.; Svedström, K.; Duša, F.; Ahvenainen, P.; **Ruokonen, S.-K**.; Witos, J.; Wiedmer, S.K., Effects of phosphonium-based ionic liquids on phospholipid membranes studied by small-angle X-ray scattering. *Chemistry and Physics of lipids,* 2016, 201, 59–66.

Witos J.; Russo, G.; **Ruokonen S.-K**.; Wiedmer S.K., Unraveling interactions between ionic liquids and phospholipid vesicles using nanoplasmonic sensing. *Langmuir* 2017, 33, (4), 1066–1076.

Robciuc A.; Witos J.; **Ruokonen S.-K**.; Rantamäki A.H.; Pisella P.-J.; Wiedmer S.K.; Holopainen J.M., Glaucoma drugs are toxic to human corneal epithelial cells – toxicity is not related to drug hydrophobicity. *Cornea,* 2017, 36, (10), 1249–1255.

ABBREVIATIONS

BGE	Background electrolyte
CAM	Contact angle meter
CE	Capillary electrophoresis
CHO	Chinese hamster ovary cells
Chol	Cholesterol
CMC	Critical micelle concentration
DLS	Dynamic light scattering
DNA	deoxyribonucleic acid
DOSY	Diffusion ordered spectroscopy
dpf	Days post fertilization
DPPC	1,2-dipalmitoyl-*sn*-glycero-3-phosphocholine
DSC	Differential scanning calorimetry
EC_{50}	Median effective concentration
E. coli	*Escherichia coli*
EKC	Electrokinetic chromatography
EOF	Electroosmotic flow
GHS	Globally Harmonized System of classification and labelling of chemicals
GUV	Giant unilamellar vesicle
HCE	Human corneal epithelial cells
HSAB	Hard-soft acid-base theory
IL	Ionic liquid
LEKC	Liposome electrokinetic chromatography
LUV	Large unilamellar vesicle
NMR	Nuclear magnetic resonance spectroscopy
MEKC	Micellar electrokinetic chromatography
MLV	Multilamellar vesicle
mpf	Months post fertilization
OECD	Organization for Economic Co-operation and Development
PC	Phosphatidylcholine
PE	Phospatidylethanolamine

PFG	Pulsed field gradient
PG	Phospahtidylglycerol
PI	Phospahtidylinositol
POPC	1-palmitoyl-2-oleoyl-*sn*-glycero-3-phosphocholine
POPG	1-palmitoyl-2-oleyl-*sn*-glycero-3-phospho-(1'-*rac*-glycerol) (sodium salt)
PS	Phosphatidylserine
PSP	Pseudostationary phase
RBC	Red blood cells
REACH	Registration, Evaluation, Authorization, and Restriction of Chemicals
RNA	Ribonucleic acid
SD	Standard deviation
SEM	Standard error of the mean
SM	Sphingomyelin
SUV	Small unilamellar vesicle
V. fischeri	*Vibrio fischeri*
ZP	Zeta potential

SYMBOLS

C_p	Heat capacity $[\frac{kg \cdot m^2}{K \cdot s^2}]$
c_{PSP}	PSP concentration $[\frac{mol}{L}]$
D	Diffusion constant $[\frac{m^2}{s}]$
G	Gradient pulse strength $[\frac{T}{m}]$
I	Signal Intensity after a gradient
I_s	Ionic strength $[\frac{mol}{L}]$
I_0	Initial signal intensity
K_D	Distribution constant
k	Retention factor
k_B	Boltzmann constant $[\frac{J}{K}]$
L_{det}	Length to the detector $[m]$
L_{tot}	Total capillary length $[m]$
M	Molar mass $[\frac{g}{mol}]$
q	Charge of an analyte
R_H	Hydrodynamic radius $[m]$
r	Radius of an analyte $[m]$
s_o or L_β	Ordered crystalline solid state
T	Temperature $[K]$
T_M	Main phase transition temperature $[K]$
t_m	Migration time of an analyte $[s]$
U	Voltage $[V]$
V_{aq}	Volume of the aqueous phase in a capillary $[L]$
V_{PSP}	Volume of the PSP in a capillary $[L]$
γ	Gyromagnetic ratio of the nucleus $[\frac{rad}{s \cdot T}]$
Δ	Delay time $[s]$
δ	Durations of the gradient pulse $[s]$
ζ	Zeta potential $[V]$

η	Viscosity of BGE $[\frac{kg}{s \cdot m}]$
μ_{tot}	Total electrophoretic mobility of an analyte $[\frac{m^2}{V \cdot s}]$
μ_{EOF}	Electroosmotic flow mobility $[\frac{m^2}{V \cdot s}]$
μ_{eff}	Effective electrophoretic mobility of an analyte $[\frac{m^2}{V \cdot s}]$
μ_0	Effective electrophoretic mobility of an analyte in CZE $[\frac{m^2}{V \cdot s}]$
μ_{LECK}	Effective electrophoretic mobility of an analyte in LEKC $[\frac{m^2}{V \cdot s}]$
μ_{PSP}	Effective electrophoretic mobility of the PSP $[\frac{m^2}{V \cdot s}]$
Φ	Phase ratio

1. INTRODUCTION

Ionic liquids (ILs) are most commonly defined as organic salts having melting points below 100 °C. They possess excellent physical and chemical properties, thus they are widely used in a myriad of studies. Because of their use in many green applications[1-3] and due to their negligible release in the atmosphere via evaporation, they are often quoted as “green solvents”. However, many classes of ILs are water-soluble as well as lipophilic and they can end up in the aqueous ecosystem through accidental spills and drains. They are also potential soil contaminants. Moreover, due to the high number of possible IL structures, not all ILs are biodegradable. The properties that make them suitable for many applications, such as high chemical and thermal stability and non-volatility can promote the ILs to bioaccumulate into small aquatic and terrestrial organisms. ILs can furthermore be transferred to animals in higher trophic levels in a food chain, and eventually even to humans.[4, 5]

For “thorough” studies on the toxicity of ILs, models consisting of animal tests with species close to humans are typically used. These tests follow commonly the official Registration, Evaluation, Authorization, and Restriction of Chemicals (REACH) guidelines approved by the Organization for Economic Co-operation and Development (OECD) and the European Union, and offer information on how different exposure methods such as inhalation, skin contact, intravenous, and oral exposure *etc.* affect the test object.[6] Usually in toxicity screening, when an amount of dose is of interest, invertebrates, plants, or various cell lines are suitable test objects. However, these methods are often targeted tests providing information on one property, such as the lethal concentration range of the studied compound.[7]

Due to the many possible structural possibilities of ILs, it is clear that the ILs exert toxicity by different means. Like other small compounds,[8, 9] non-surface-active ILs might be absorbed through the plasma membrane without causing any effect to the membrane itself[10] or they might interact with cells by binding to receptors and furthermore by inducing an intracellular responses.

The surface-active ILs, on the other hand, can penetrate the plasma membrane, thus, the interdependency of hydrophobicity and toxicity of ILs is largely adopted in many studies.[11-15] The intercalation capability of the surface-active ILs into cell membranes are known to affect the IL toxicity, therefore many studies have used liposomes as membrane biomimicking models.[16, 17] The surface-active ILs are speculated to enhance the facilitated uptake of a compound into an organism, leading to an increased internal toxicant concentration and to an altered metabolism. Another hypothesis is that IL-induced perturbation and decrease of membrane order might affect the ion and/or molecule transportation through the membrane.[18] However, it is evident that the toxicity increases when adsorbed or absorbed hydrophobic moieties of ILs compromise the membrane

integrity. Because of many possible IL classes and combinations it is impossible to predict one exact mechanism of toxicity for all ILs.

The aim of this PhD work was to elucidate the effect of the IL structure on the toxicity using zebra fish and different cell lines as test organisms. Furthermore, this data was utilized to find novel methodologies for assessing IL toxicity using biomimicking liposomes.

The study addresses:

- the effect of ILs on zebrafish viability, behavior, and histology and compare the results with cytotoxicity information (paper I)
- the cytotoxicity of ILs and determine the influence of long-chained phosphonium-based ILs on the size and zeta potential of L-*α*-phosphatidylcholine from egg yolk (eggPC)/ 1-palmitoyl-2-oleyl-*sn*-glycero-3-phospho-(1'-*rac*-glycerol) (sodium salt) (POPG) (75/25 mol%) liposomes with and without cholesterol (paper II)
- the effect of liposome composition and temperature on the distribution of local anesthetics between aqueous and liposome phases (paper III)
- how the permeation of surface active ILs into liposomes are connected with the cytotoxicity of the ILs (paper IV)
- how the aggregation of ILs affects the IL-biomembrane interactions (papers I, II and IV)
- the cytotoxicity of ILs through IL-liposome interactions (paper V)

2. BACKGROUND

2.1. Ionic liquids

The first publications concerning the low melting points of organic salts were published in the early 20th century.[19, 20] Since then many names have been used for ILs and IL-like-substances such as, molten salts, fused salts, ionic melts, ionic fluids, and liquid electrolytes[21-23] before the term "ionic liquid" became the most used in 1940–1950.[24, 25] Synthetic procedures for approximately 10^3 IL pairs have been reported[4], however, it has been estimated that approximately 10^6 possible simple IL pairs are accessible.[20] Hence, ILs are quoted as designer solvents due to the possibility to alter the chemical and physical properties of the compounds via appropriate selection of the cation and anion pair. Ionic bonds of ILs enable high miscibility with polar substances, while the presence of alkyl chains determines the miscibility in less polar substances, thus, making ILs excellent solvents for a wide range of componds.[26] Usually ILs consist of asymmetric organic imidazolium-, pyridinium-, ammonium-, pyrrolidinium-, phosphonium-, piperidinium-, morpholinium-, or cholinium-based cations and inorganic halide (Cl^-, Br^-, I^-), triflate $[TfO]^-$, bis(trifluoromethylsulfonyl)imide $[NTf_2]^-$, tetrafluoroborate $[BF_4]^-$, hexafluorophosphate $[PF_6]^-$, or acetate $[OAc]^-$ anions. Typical features of ILs are low flammability, low vapor pressures (often 10^{-11}–10^{-10} mbar), and low melting points (<100 °C).[4, 5, 27] These easily tunable properties make the ILs widely utilized in many industrial, pharmaceutical[28], and commercial applications and they are nowadays produced at industrial scale in many companies, *e.g.*, at BASF[29] and IoLiTec[30]. ILs are commonly used in organic synthesis[31] and catalysis[32], analytical chemistry[33], food industry[34], biomass processing[35, 36], and as electrolytes[37], to mention a few. Due to their wide range of applications, the toxicity of ILs is becoming a general concern for a wide number of users.

2.1.1 Ionic liquid toxicity

When assessing the greenness of ILs one should consider the whole life cycle from synthesis to disposal. The synthesis and purification of ILs are not always green,[38] thus, the twelve general principles of Green Chemistry should be followed.[39] The number of toxicity studies of ILs has drastically risen since year 2000, as the use and design of "green" ILs has become paramount. Most of the toxicity studies (published prior to March 2015) used *in vitro* models (18%) or marine bacteria (15%), while *in vivo* studies using whole mammals covers approximately 8% of the toxicity studies.[21] Recently, also *in vitro* tests using human skin have been published.[40] The main factors affecting the toxicity are (1) the cation alkyl chain length, (2) the degree of functionalization of the side chain of the cation, (3) the nature of the anion, (4) the nature of the cation, and (5) the mutual influence of anions and cations. In addition to these IL properties, the test organism and the IL environment

(solvent, pH, matrix, temperature *etc*.) influence the observed results.[41 27, 42] It has also been shown that whether the IL cation is protic or not, appear to be secondary to the effect of the cation functional group.[43] The degradation of ILs is the major factor affecting the disposal and/or repository of ILs after use, hence, many toxicological studies are concentrated on this aspect.[42]

ILs are often quoted as “designer solvents” due to many possible IL structures. Thus, the mechanism of toxicity varies from one structure to another. ILs can be roughly divided to non-surface-active and surface-active ILs based on their capability to reduce surface tension. The non-surface-active ILs are usually relatively small (<500–600 g/mol) and can penetrate the cell plasma membrane without comprising the bilayer integrity (*transcellular permeability*). Yet, all ILs are charged and it is plausible that these compounds enter tissues using intercellular aqueducts for transportation (*paracellular permeability*), via suitable transporters or they do not enter the cells but bind to receptors which can induce subcellular responces.[9, 44] The ILs can be harmful in their preliminary forms or they can undergo metabolism and become more or less toxic, hampering the determination of the mechanism of toxicity.[45] For example, 1-butyl-3-methylimidazolium cation has been predicted to break down to biocompatible fatty acids and imidazole cation if they reach the cytochrome P450 in endoplasmatic reticulum.[46] Surface-active ILs have been speculated to permeate into the membrane, saturating the membrane[47] and inducing roughening[48] and/or swelling[13] of the membrane. It has been shown, that when the surfactant concentration exceeds the saturation concentration phospholipid vesicles rupture forming smaller surfactant-lipid micelles, which co-exist with surfactant-lipid vesicles.[49, 50] Jing *et al.* have shown that surface-active imidazolium-based ILs interact with eggPC liposomes in a similar manner forming IL-lipid micelles.[13] In addition, imidazolium and cholinium-based ILs with a lactate anion[51] and imidazolium-, pyrrolidinium-, and pyridinium-based ILs[16] have been shown to induce liposome fusion of zwitterionic liposomes.

ILs can be divided into hard or soft electrophiles based on the hard-soft acid-base theory (HSAB theory).[52] Phosphonium and cholinium-based IL can be categorized as hard electrophiles and therefore they prefer to interact with hard nucleophiles such as deoxyribonucleic acid and ribonucleic acid (DNA and RNA, respectively) and are plausibly prone to cause cancer. The imidazolium and amidinium IL cations, on the other hand, can be considered as soft electrophiles and prefer to interact with proteins, thus they are prone to cause organ damage. It has been shown before, that imidazolium-based ILs can inhibit trypsin activity,[53] acetylcholinesterase enzymes,[54] and adenosine monophosphate (AMP) deaminase activity,[55] which supports the HSAB hypothesis. In addition, metabolic degradation of ILs can affect their toxicity.

2.2 Zebrafish

Fish are located in high trophic level in an aquatic food chain, therefore the use of fish, when evaluating the ecotoxicity of toxicants on the aquatic environment, is essential. Zebrafish are widely used model organisms for toxicity assessments. They are transparent, easy to maintain, relatively inexpensive and the embryos have rapid development (Figure 1).

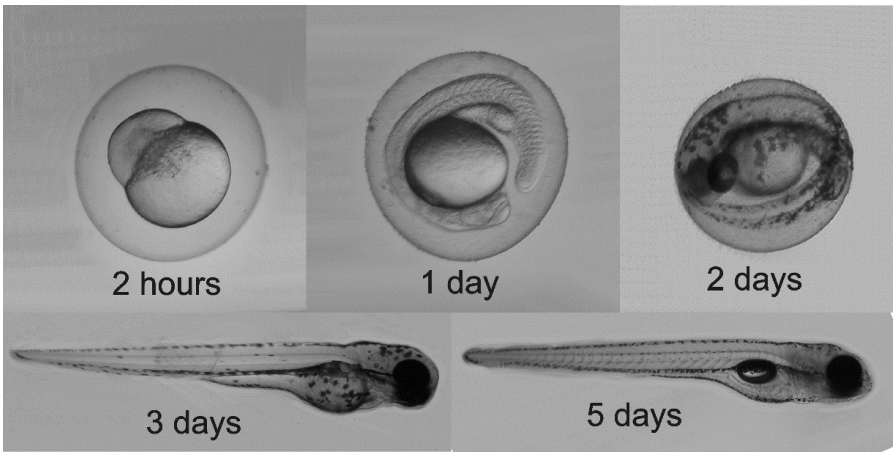

Figure 1. Development of Zebrafish within five days post fertilization. Adapted with permission from "Ruokonen, S.-K., *et al*., 2016, *Environ. Sci. Technol.,* 50, (13), 7116-7125." Copyright (2018) American Chemical Society.

In addition to toxicant viability tests, zebrafish can be used for evaluating long-term exposure impacts of toxicants. These can include the assessment of the offspring of the exposed fish or evaluation of the long-term exposure on behavior, histology or phenotype of the fish.[56, 57]

2.3 Cytotoxicity

Two cell types, mammalian and bacterial cells, were utilized in the cytotoxicity studies. Mammalian cells have a cell nucleus enclosed in a phospholipid bilayer whereas the plasma membrane of gram negative bacteria is composed of a thin peptidoglycan network located between two phospholipid bilayers. Bacteria do not have a membrane-bound nucleus and the DNA is located irregularly in the cytosol. The structure of mammalian cells is more complex than bacterial cells. Therefore, the use of bacterial cells provides simple information on the interactions of toxicants and membranes, whereas mammalian cells are generally used to gain more detailed information on the cytotoxicity mechanism of toxicants.[8]

2.3.1 Mammalian cells

Chinese hamster ovary cells (CHO) cells and human corneal epithelial cells (HCE) are epithelial cells, which grow as adherent monolayers in cultures. The rapid growth, low chromosome number, and clear karyotype of CHO cells make them ideal models for mammalian cells. They are commonly used in biological and medical applications, especially in median effective concentration (EC_{50}) determinations and as host cells for therapeutic proteins.[58] HCE cells on the other hand, occupy the outermost layer of cornea. They are considered as good models for human cells, especially for assessing ocular drug delivery because they retain many of the characteristics of the original tissue.[59]

2.3.2 Bacterial cells

Vibrio fischeri (*V. fischeri*) are bioluminescent marine bacteria that are frequently found in symbiotic relationships with marine animals. The bioluminescence arises when luciferin is oxidized via the help of the luciferase enzyme.[60] When the bacteria are exposed to an external toxicant, the bioluminescence decreases and the decay is proportional to the EC_{50} value. The commercial method (Microtox) utilizing *V. fischeri* is a widely used for assessing aquatic toxicity because it is simple, fast, and well established.[61-66]

Escherichia coli (*E. coli*) bacteria are commonly located in the intestines of animals and humans. They are usually harmless, however some strands are pathogenic and can cause illness. *E. coli* is an extensively studied prokaryotic model organism in the field of biotechnology and microbiology, mainly because the bacteria can be grown easily and inexpensively in a laboratory setting.[67] It has been intensively studied for over 60 years and is nowadays widely used in the assessment of IL toxicity.[68-70]

2.4 Liposomes

Liposomes are spherical vesicles comprising lipid bilayers enclosing an aqueous compartment. Bilayer forming phospholipids self-assemble to multilamellar vesicles (MLV, Figure 2A) generally at low concentrations (10^{-6}–10^{-9} M).[71] The nonpolar, hydrophobic tails are aligned inwards and the polar, hydrophilic tails are aligned outwards in aqueous solutions. They can be further modified to small (20–100 nm), large (100 nm–1 μm), or giant (>1 μm) unilamellar vesicles (SUV, LUV, and

GUV, respectively, Figure 2B) to model simple cell membranes. Liposomes are used in several application as biomimicking membranes, signal transduction, or as drug delivery vehicles.[71-73]

The most abundant phospholipids in cell membranes are phosphatidylcholine, phosphatidylethanolamine (PE), phosphatidylinositol (PI), phosphatidylserine (PS), phosphatidylglycerol (PG), and sphingomyelin (SM). Their composition vary depending on the tissue, however, usually PC is the main component.[74] In addition to phospholipids, eukaryotic cell membranes contain approximately 20 to 50 mol% of cholesterol. The hydroxyl groups of cholesterol are positioned close to the polar phospholipid head groups and the hydrophobic steroid rings are located near the lipid acyl chains, making the membrane region more rigid. These cholesterol-rich domains are sometimes called rafts and they are less fluid than the surrounding cholesterol-poor regions decreasing the passive permeability of small molecules into the membrane. [75-80]

Cell membranes are defined as two-dimensional liquids that undergo phase transitions as a function of temperature.[77] These phase transitions involve a change in the order of the system. The main phase transition *i.e.,* the chain-melting-transition occurs when the highly ordered crystalline solid state (s_o or L_β), the so-called gel state, is transformed into a disordered liquid state (l_d or L_α), *i.*e., to the fluid state (Figure 2C). In cholesterol-rich domains ordered liquid state (l_o) can occur and coexist with the l_d state.[75, 77, 78]

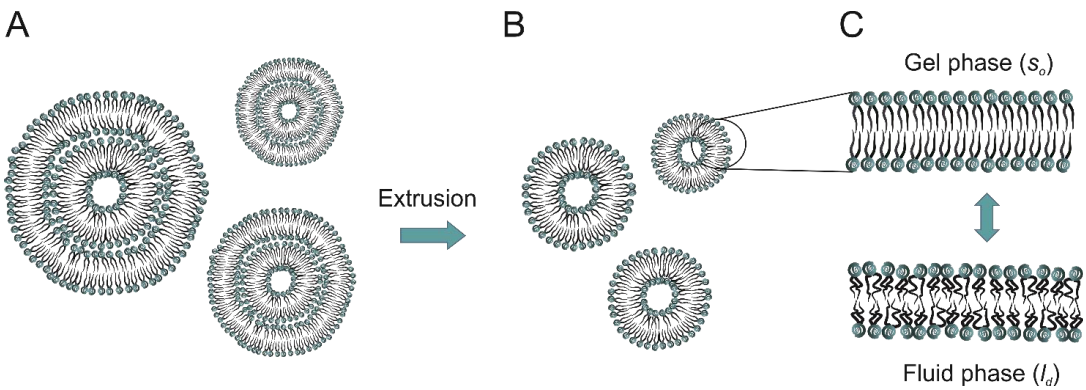

Figure 2. A) Multilamellar vesicles, B) unilamellar vesicles, and C) phase transition of a lipid bilayer from the ordered gel phase to the disordered fluid phase.

2.5 Aggregation of ionic liquids

The transition from the unimeric form to an aggregated form does not always occur at a sharply defined concentration. The widely accepted definition (Phillips definition)[81] of the critical micelle

concentration (CMC) states that the CMC corresponds to the concentration range where the maximum change in the physical property of the surface-active compound (surfactant) such as electrical conductivity, surface tension, osmotic pressure, density, light scattering, or refractive index[82, 83] appears. However, nowadays the CMC is often defined as the concentration, above which the aggregates are formed in a solution.[84] Aggregates are formed when amphiphilic monomers aggregate, with the nonpolar hydrophobic moieties aligned inwards and the polar hydrophilic moieties aligned outwards, in an aqueous solution. The aggregates can have various structures such as ellipsoidal, cylindrical or disklike micelles, spherical micelles, bilayers, or vesicles.[85] Many ILs are surfactants and the possible aggregate formation of ILs may have an impact on the synthesis, purification, and solvation properties of the compounds.[86] Furthermore, the lipophilicity of IL unimers and aggregates may differ, which may change their interactions with organisms.

3. METHODOLOGIES

3.1 Microtox bioassay

The Microtox bioassay is used for *in vitro* toxicity assessment *i.e.,* for the determination of the median effective concentration of various solids and liquids. The assay measures the bioluminescence decay of *Vibrio fischeri* marine bacteria in the presence of exogenous toxicants at different concentrations. The bacteria are freeze-dried prior to use, which enables their easy and rapid use in toxicity assessments. Three main substrates are involved in the bioluminescence process: the reduced flavine mononucleotide (FMN) and a long chained aldehyde from the bacterial metabolism and dissolved oxygen from the environment.[87] The bioluminescence arises when luciferin molecule or molecules ("the light bearing molecule" *i.e.,* the aldehyde and the FMN) are oxidized with the help of the luciferase enzyme, after which they are again reduced with the assistance of a catalysts,[88] shown in Scheme 1.

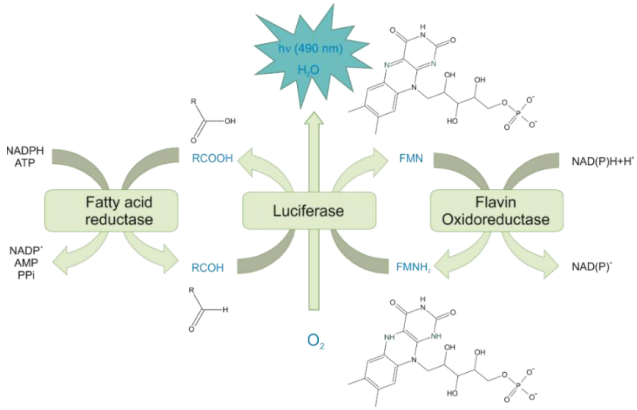

Scheme 1. Arise of bioluminescence of *V. fischeri* bacteria. Adapted from references 87,88, and 89.

When the bioluminescent process is interfered by an exogenous compound, the intensity of the bioluminescent decreases. The toxicant may affect *e.g.*, the energy transfer processes of the bioluminescence (electron excited state population and conversions), the rate of the reactions, the electron density distribution, or the enzymatic activity of the enzymes involved in the reactions.[60]

3.2 Capillary electrophoresis

Capillary electrophoresis (CE) is a separation technique, in which the analytes are separated according to their charge to size ratio. A voltage is applied between two electrodes and an electric field is created in a fused silica capillary filled with a background electrolyte (BGE) solution. The CE set up is shown in Figure 3. The silica capillary wall is negatively charged at pH values higher than two. When a voltage is applied a double layer is formed due to electrostatic interactions between the dissociated silanol groups of the fused silica capillary wall and the BGE cations. The double layer consists of an immobile Stern layer closest to the capillary surface and a loosely adsorbed diffuse layer. In normal mode (positive polarity), the loosely bound cations start to migrate towards the cathode forming a bulk flow *i.e.*, an electroosmotic flow (EOF).[90] Thus, the total electrophoretic mobility of an analyte under the influence of the electric field (μ_{tot}, Equation 1) is the sum of the EOF mobility (μ_{EOF}) and its own effective electrophoretic mobility (μ_{eff}, Equation 2), which depends on the analyte charge (q), radius (r), and the solution viscosity (η).

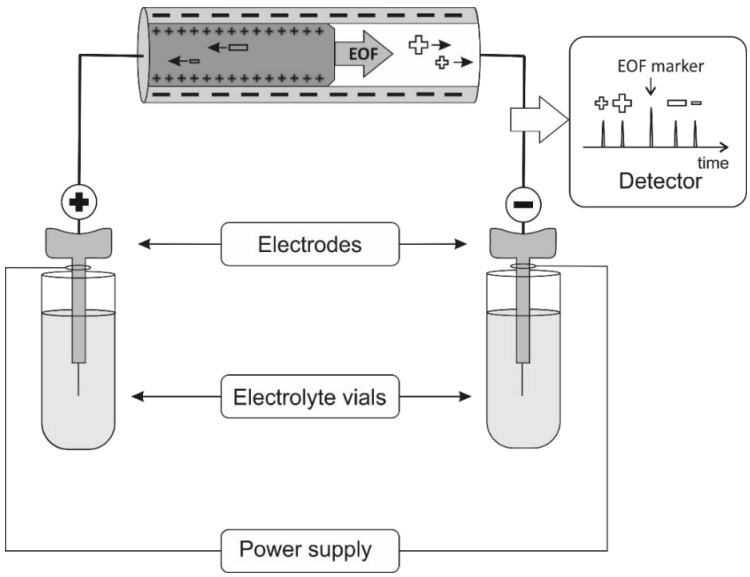

Figure 3. Instrumental set up of CE.

$$\mu_{tot} = \mu_{EOF} + \mu_{eff} \quad (1)$$

$$\mu_{eff} = \frac{q}{6\pi\eta r} \quad (2)$$

The μ_{tot} can be calculated from Equation 3, once the migration time (t_m) of the analyte is determined experimentally.

$$\mu_{tot} = \frac{L_{tot} \cdot L_{det}}{U \cdot t_m} \quad (3)$$

CZE as such, is not a suitable separation technique for uncharged analytes, which migrate with the same mobility due to the influence of the EOF. However, electrokinetic chromatography (EKC), which is a sub-technique of CE, can be utilized for the separation of uncharged analytes. In EKC the silica capillary is filled with a hydrophobic pseudostationary phase (PSP) commonly comprising surfactant micelles (micellar elektrokinetic chromatography, MEKC). Additionally the PSP can consist of nanoparticles such as nanotubes or graphene[91], ionic polymers[92] or liposomes (liposome electrokinetic chromatography, LEKC), to mention a few. In addition of separating neutral analytes, LEKC has been recognized as a good method for studying interactions between compounds and liposomes.[93, 94]

In EKC, in addition to the effective electrophoretic mobility and the EOF, the total mobility of an analyte is dependent on its partitioning between the aqueous phase and the hydrophobic PSP. The latter chromatographic part of the mobility is dependent on both the hydrophobicity and the surface charge of the analyte.

The retention factor (k) of an analyte under EKC conditions can be calculated using Equation 4,

$$k = \frac{\mu_{EKC} - \mu_0}{\mu_{PSP} - \mu_{EKC}} \quad (4)$$

where the μ_{EKC} and μ_0 are the effective electrophoretic mobilities of an analyte under EKC and CE conditions, respectively and μ_{PSP} is the effective electrophoretic mobility of the PSP. The retention factor elucidates the mole ratio of the analyte between the PSP and the aqueous phase.[95] The distribution constant (K_D), on the other hand, is the molar concentration ratio of the analyte between the PSP and the aqueous phase and elucidates the analyte-liposome interaction in systems with various concentrations of PSP.[96] K_D values can be calculated for systems with known phase ratios (Φ) at different temperatures using Equation 5.

$$K_D = \frac{k}{\Phi} \quad (5)$$

Φ is the volume ratio of the liposomes (V_{PSP}) and the aqueous phase (V_{aq}) in the capillary and can be calculated according to Equation 6.

$$\Phi = \frac{V_{PSP}}{V_{aq}} = \frac{\nu_{spec,vol} \cdot M \cdot (c_{PSP} - CMC)}{1 - (\nu_{spec,vol} \cdot M \cdot (c_{PSP} - CMC))} \quad (6)$$

$\nu_{spec,vol}$ is the partial specific volume and M is the molar mass of the PSP unimer, c_{PSP} is the total concentration of the PSP, and CMC is the critical micelle concentration of the PSP micelle/vesicle in the dispersion.

3.3 Dynamic light scattering

In dynamic light scattering (DLS) the change in the light intensity, scattered from a particle is determined. When the particle diffuses spontaneously in a solution (Brownian motion) the scattered light undergoes either a constructive or a destructive interference, causing a fluctuation in the light intensity when it passes the detector. This change in the light intensity is dependent on the velocity of the particle diffusion – small particles cause the intensity to fluctuate more rapidly than larger ones. When the intensity fluctuation is correlated against short decay intervals, an autocorrelation function is obtained and the particle radius can be determined using the Stokes-Einstein equation (Equation 7).[97, 98]

$$D = \frac{k_B \cdot}{6\pi \cdot \eta \cdot R_H} \quad (7)$$

D is the diffusion constant of the particle, k_B is the Boltzmann constant, T is the temperature, η is the viscosity of the solvent, and R_H is the hydrodynamic radius of the particle.

3.4 Zeta potential measurements

In an aqueous solution, a double layer, consisting of a Stern layer and a diffuse layer, is formed around a charged particle. When an electric field is applied to the system, the charged particles, with the adsorbed double layer, move toward the electrode of opposite charge. A hypothetical plane is located within the diffuse layer (slipping plane), which acts as the interface between the mobile layer

moving with the particle and the immobile layer of the solvent around it. The zeta potential (ζ) is the potential at this point (Figure 4) and it is determined from the electrophoretic mobility of the particle.[99]

The zeta potential of a particle can be measured by determining its electrophoretic mobility, which is

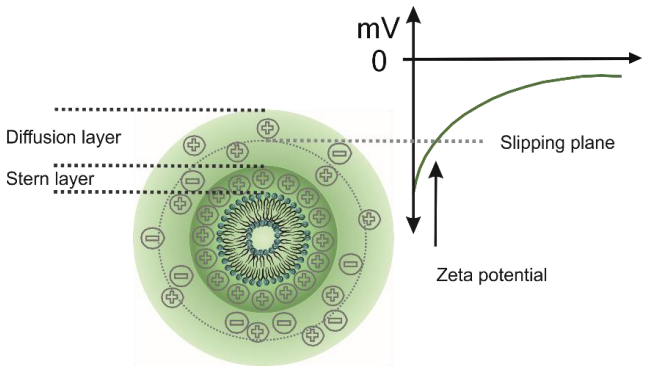

Figure 4. Negatively charged particle in an electric field.

directly proportional to the zeta potential. First, the incident light beam passes through the sample and when an electric field is applied the movement of the particle changes the frequency of the scattered light. The scattered light, which frequency shift is proportional to the electrophoretic mobility is combined with the reference beam and the zeta potential of a particle is determined.[97, 100]

3.5 Differential scanning calorimetry

Differential scanning calorimetry (DSC), *i.e.,* microcalorimetry, is a technique that measures thermodynamic properties of thermally induced transitions in substances, which require or release energy. These include conformational changes of macromolecules, binding to proteins, lipid phase transitions etc.[101] DSC has two cells, a sample cell and a reference cell. The energy required to maintain the cells at the same temperature while the sample undergoes a phase transition or conformational change, is measured by measuring the isobaric heat capacity difference (ΔC_p) between the cells.[102, 103] DSC can be used for assessing the order of the lipid bilayer in the presence of external toxicants. In liposomes, a phase transition occurs when a lipid bilayer undergoes a gradual transformation from an ordered gel phase to a disordered fluid phase, or vice versa, within a short temperature range. If the lipid bilayer is perturbed with an external surface-active toxicant, the lipid order is reduced and its phase transition temperature is decreased. In addition, DSC can be used for monitoring the rupturing of a lipid bilayer by following the disappearance of the signal — when there is no intact bilayer in the system undergoing phase transition, no signal occurs.

3.6 Optical pendant drop method

The optical pendant drop method is a useful method for CMC determinations. A drop is formed using a contact angle meter (CAM) and the shape of the drop is dependent on the surface tension.[104] Images of the drop are captured using a camera and a suitable fitting function is applied to the drop image to determine the surface tension. When a surface-active compound is added to the sample, the unimers orientate at the surface of the drop in order to decrease the free energy of the system. The surface tension decreases until the surface of the drop is fully covered and the system reaches a balance. When the concentration is increased all additional unimers aggregate and the surface tension reaches a relatively constant value. The CMC is determined by plotting the surface tension as a function of the logarithm of the sample concentration, and defining the value at the intersection point of two trend lines.

3.7 Nuclear magnetic resonance spectroscopy

NMR is the one of the most used analytical techniques for the determination of molecular structures.[105] Pulsed field gradient (PFG) NMR, and especially diffusion ordered spectroscopy (DOSY), is used to determine molecular displacement and can be utilized for assessing the size of a molecule, degree of polymerization, or the size of a solvation shell. A series of echo spectra are measured with different pulsed field gradient strengths. The pulse gradients create phase shifts that depend on the spatial position of the spins. A second opposite gradient is used to return the spins in-phase. However, the new molecular position, due to diffusion between the pulses, lead to a decrease in the NMR signal intensity. This decay is dependent on the gradient pulse strength (G) and duration (δ), and the diffusion constant (D) can be determined by following the signal decays.[106] The signal intensity (I) is attenuated with respect to the signal in the absence of a gradient (I_0) as

$$\frac{I}{I_0} = \exp(-\gamma^2 \delta^2 G^2 D(\Delta - \frac{\delta}{3}) \quad (8)$$

where γ is the gyromagnetic ratio of the nucleus and Δ is the delay time. Furthermore, the hydrodynamic radius of the diffusing aggregates can be estimated from the Stokes-Einstein equation (Equation 7) described in section 3.3.

4. EXPERIMENTAL

All used ionic liquids (Table 1), lipids (Table 2), chemicals and substances (Table 3), organisms (Table 4), and instruments and materials (Table 5) used in the studies (I–V) are listed below.

4.1. Materials and methods

Table 1. List of ionic liquids used in the studies.

Ionic liquid	Abbreviation	Manufacturer	Paper
1,5-Diazabicyclo(4.3.0)non-5-enium acetate	[DBNH][OAc]	Synthesized[107]	I, II, V
1-Ethyl-3-methylimidazolium acetate	[emim][OAc]	IoLiTec, GmbH	I, II, V
1-Ethyl-3-methylimidazolium chloride	[emim]Cl	IoLiTec, GmbH	II
1-Ethyl-3-methylimidazolium dimethylphosphate	[emim][Me_2PO_4]	Synthesized[108]	II
1-Ethyl-3-methylimidazolium methylhydrogenphosphonate	[emim][$MeHPO_3$]	Synthesized[108]	II
Choline acetate	[Ch][OAc]	Synthesized*	V
Cholinium hexanoate	[Ch][Hex]	Synthesized*	V
Cholinium decanoate	[Ch][$C_9H_{19}COO$]	Synthesized**	IV
Cholinium isostearate	[Ch][$C_{17}H_{35}COO$]	Synthesized**	IV
Cholinium neodecanoate	[Ch][Neo-$C_9H_{19}COO$]	Synthesized**	IV
Guanidinium isostearate	[GND][$C_{17}H_{35}COO$]	Synthesized**	IV
Guanidinium neodecanoate	[GND][$C_9H_{19}COO$]	Synthesized**	IV
Isostearic acid		Pristorine™ 3501, Croda Internatinal Plc.	IV
Methyltributylammonium acetate	[N_{4441}][OAc]	Synthesized*	V
Neodecanoic acid		Hexion Speciality Chemicals	IV
Octyltributylphosphonium chloride	[P_{8444}]Cl	Cytec Industries	II
Sodium decanoate	Na[$C_9H_{19}COO$]	Synthesized**	IV
Sodium Isostearate	Na[$C_{17}H_{35}COO$]	Synthesized**	IV
Sodium neodecanoate	Na[Neo-$C_9H_{19}COO$]	Synthesized**	IV
Tetrabutylphoshonium chloride	[P_{4444}]Cl	Cytec Industries	II
Tetrabutylphosphonium acetate	[P_{4444}][OAc]	Synthesized[35]	I, II
Tetramethylguanidinium isostearate	[GND][$C_{17}H_{35}COO$]	Synthesized**	IV
Tetramethylguanidinium neodecanoate	[TMG][$C_9H_{19}COO$]	Synthesized**	IV
Tributyl(tetradecyl)phosphonium acetate	[P_{14444}][OAc]	Synthesized[35]	I, II, V

Table 1. Continued

Ionic liquid	Abbreviation	Manufacturer	Paper
Tributyl(tetradecyl)phosphonium chloride	$[P_{14444}]Cl$	Cytec Industries	II, V
Tributylmethylphosphonium acetate	$[P_{4441}][OAc]$	Synthesized***	I, V
Tributylmethylphosphonium decanoate	$[P_{4441}][C_9H_{19}COO]$	Synthesized***	I
Tributylmethylphosphonium hexadecanoate	$[P_{4441}][C_{15}H_{31}COO]$	Synthesized***	I
Tributylmethylphosphonium hexanoate	$[P_{4441}][C_5H_{11}COO]$	Synthesized***	I
Tributylmethylphosphonium methyl carbonate	$[P_{4441}][CH_3OCOO]$	IoLiTec, GmbH	I
Tributylmethylphosphonium octadecanoate	$[P_{4441}][C_{17}H_{35}COO]$	Synthesized***	I
Tributylmethylphosphonium tetradecanoate	$[P_{4441}][C_{13}H_{27}COO]$	Synthesized***	I
Tributyloctylphosphonium acetate	$[P_{8444}][OAc]$	Synthesized****	I, II
Trihexyl(tetradecyl)phosphonium acetate	$[P_{14666}][OAc]$	Synthesized[35]	II

*Paper V, **Paper IV, ***Paper I, ****Paper II

Table 2. List of lipids used in the studies.

Lipids	Abbreviation	Manufacturer	Paper
1,2-dipalmitoyl-sn-glycero-3-phosphocholine	DPPC	Avanti Lipids	IV, V
1-palmitoyl-2-oleoyl-*sn*-glycero-3-phosphocholine	POPC	Avanti Lipids	III
1-palmitoyl-2-oleyl-*sn*-glycero-3-phospho-(1'-*rac*-glycerol) (sodium salt)	POPG	Genzyme Pharmaceuticals	II, III
Cholesterol	Chol	Avanti Lipids	II, III
L-α-phosphatidylcholine (egg, chicken)	eggPC	Avanti Lipids	II, V
L-α-phosphatidylglycerol (Egg, Chicken; eggPG) (sodium salt)	eggPG	Avanti Lipids	V
Red blood cell lipids	RBC	Extracted in-house[109]	III

Table 3. List of chemicals and substances used in the studies.

Chemical or substance	Manufacturer	Paper
Acetic acid	Sigma-Aldrich	II
alamarBlue dye	Invitrogen Thermo Fischer Scientific	I, II V
Alkyl benzoates	Sigma	III
Ampicillin sodium salt	AppliChem	II
Anesthetics	Gift from Prof. Mohamed Abdel-Rehim	III
Calcium chloride dehydrate	Sigma	I
CellTox™ Green dye	Promega, Madison, WI	V
Chloroform	Rathburn WVR International	II–V
Cholera toxin	Sigma-Alrich-Merck	V
Decanoic acid	Sigma-Aldrich	I
Deuterated water (D_2O)	Euriso-Top	V
1,5-Diazabicyclo(4.3.0)-non-5-ene (DBN)	Fluorochem Ltd.	II
Dulbecco's modified Eagle's medium (D-MEM)/F12 medium	Invitrogen Thermo Fischer Scientific	II V
Fetal bovine serum (FBS)	Invitrogen Thermo Fischer Scientific	II V
Gentamicin	Invitrogen Thermo Fischer Scientific	II V
Glutamine	Invitrogen	II
Ham’s F12	CLS cell line services GmbH	I
Ham's F12 with FBS	CLS cell line services GmbH	I
Hexanoic acid	Fluka AG (Buchs, Switzerland)	I
Human epidermal growth factor (EFG)	Invitrogen Thermo Fischer Scientific	II V
Insulin	Invitrogen Thermo Fischer Scientific	II V
Lysogeny broth (LB)	Carl Roth	II
Magnesium sulfate heptahydrate	Merck	I
Mayer’s Hemalum solution (hematoxylin) and Eosin G dye	Merck	I
Methanol	Mallinckrodt Baker Sigma	I–III V
N-methylmorpholine-N-oxide (NMMO)	Sigma	V
Paraformaldehyde PFA	Sigma	I
Phosphate buffer saline (PBS)	Life Technologies Merck	I III
Polycarbonate filter (100 nm)	Millipore	II, III
Potassium chloride	Sigma Merck	I III
Potassium dihydrogen phosphate	J. T. Baker	I, III

Table 3. Continued

Chemical or substance	Manufacturer	Paper
Sodium chloride	Riedel-de Haën	I
	Merck	III
Sodium dihydrogen phosphate monohydrate	Mallinckrodt Baker	I–III
Sodium hydrogen phosphate	Sigma	I–III
Di-sodium hydrogen phosphate dihydrate	Merck	I, III
Sodium hydroxide	FF-Chemicals	I–III
Stearic acid	Fluka AG	I
Tetradecanoic acid	Fluka AG	I
Tetradecanoic acid	Riedel-de Haën	I
The pH solutions	Merck	I–III
Thiourea	Sigma	III
Trypan blue (T8154) dye	Sigma-Aldrich	I
Trypsin/EDTA	Sigma-Aldrich	I

Table 4. List of organisms used in the studies.

Organism	Manufacturer	Paper
Chinese hamster ovary cells (CHO)-K1	CLS cell line services GmbH	I
Escherichia coli XL-1 blue bacteria	Stratagene	II
Red blood cells (RBC)	Extracted in-house[110]	V
SV-40 immortalized human corneal epithelial cells (HCE)	Helsinki Eye Lab[111]	II, V
Vibrio fischeri	Modern Water	IV, V
Zebrafish	Turku line	I

Table 5. List of instruments and materials used in the studies.

Instruments and materials	Manufacturer	Paper
0.45-µm syringe filter	Gelman Sciences	I–III
Cell culture ware	Greiner BioOne	I
	Thermo Fischer Scientific	V
Hewlett Packard ^{3D}CE	Agilent	I–III
Invert light microscope	Leica DM IRB, Leica Microsystem GmbH	I
Microtox® M500	Modern Water	IV,V
NMR spectrometer	500 MHz Bruker Avance III	V
Optical contact angle meter (CAM 200)	Biolin Scientific, KSV Instruments	I, IV
Plate reader	VERSAmax, Molecular Devices	II
	EnSpire – PerkinElmer	II, V
	Viktor^3 – PerkinElmer	I
Fused silica capillary	Polymicro Technologies	I–III
Thin layer chromatography plates	TLC silica gel 60, Merck KGaA	III
VP-DSC MicroCalorimeter	MicroCal LLC	IV, V
Zetasizer Nano ZS	Malvern Instruments Ltd	II–V
pH meter	Mettler Toledo	II, III

4.2. Preparation of samples and solutions

4.2.1. Ionic liquids

Ionic liquids used in the studies (papers I, II, IV, and V) were either commercial or synthetic and the places of purchase or the reference to the synthesis are shown in Table 1. The structures of the ILs and reference compounds are shown in Figure 5.

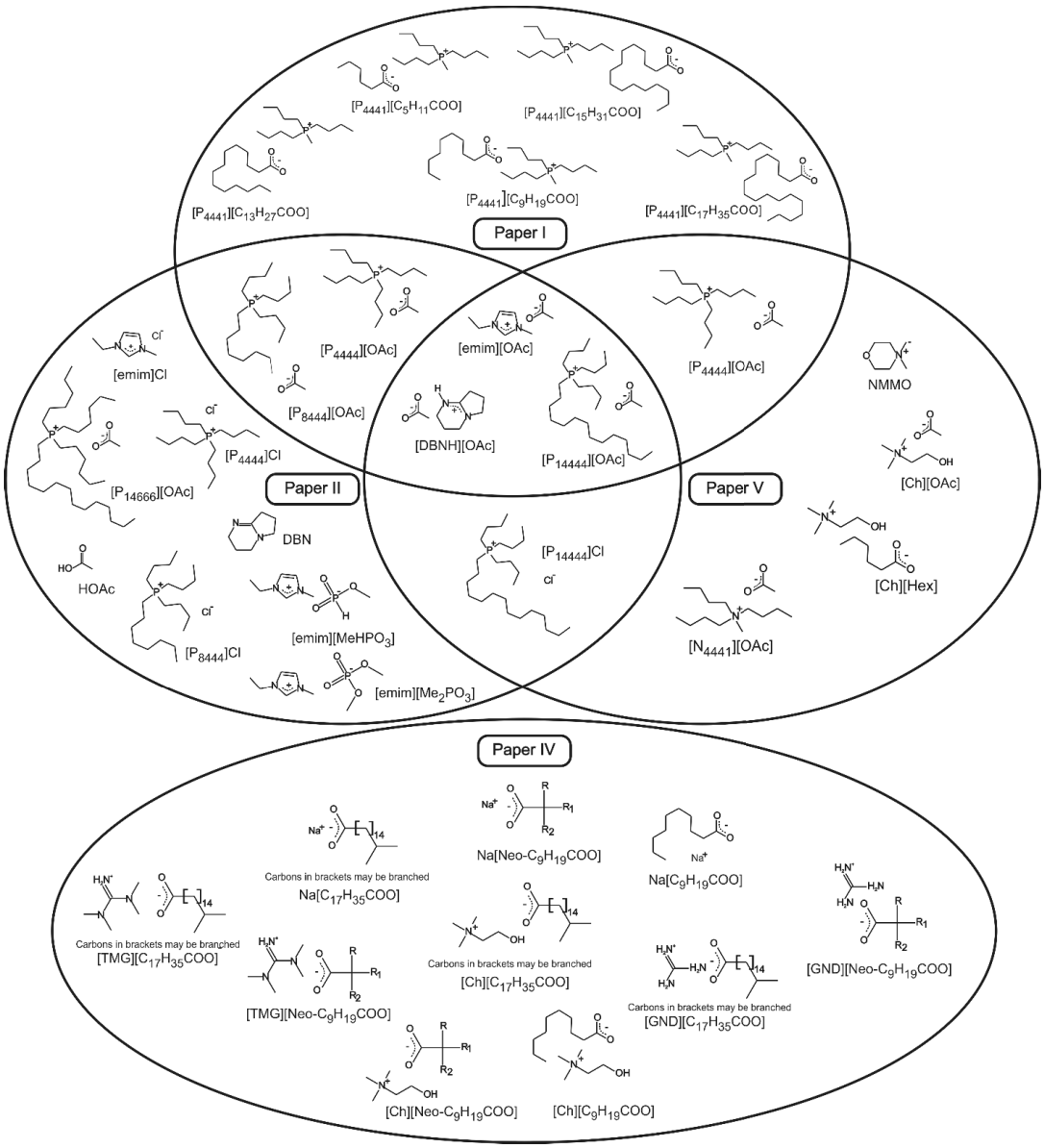

Figure 5. ILs used in Papers I, II, IV, and V.

4.2.2. Zebrafish studies

Zebrafish were fed, bred, and maintained according to an established protocol.[56] The permits for the experiments were obtained from the Office of the Regional Government of Southern Finland in agreement with the ethical guidelines of the European convention.

Zebrafish embryos from at least four different fish pairs per batch were collected right after fertilization and transferred in groups of 30 to 6-well plates containing IL solutions. Two concentrations, 1 and 100 $mg \cdot L^{-1}$ or 1 and 10 $mg \cdot L^{-1}$, were selected based on the Globally Harmonized System of classification and labelling of chemicals (GHS) classification system.[112] Each well plate contained a control group and the plates were incubated at 28 °C and illuminated for 14 hours per day. The IL solutions were changed daily and dead fish were removed from the plates. The phenotypic malformations and mortality of the embryos were noted 10 min and 24, 48, 72, 96, and 120 hours after the IL addition. All measurements were performed in triplicates (90 embryos per one IL concentration).

The swimming patterns (locomotor activity) of five days postfertilization (dpf) larvae (n>16 zebrafish per IL group) were recorded for 10 min. Long-term IL exposure effect of [DBNH][OAc] and $[P_{4441}]$[OAc] ILs on the behavior of three months postfertilization (mpf) zebrafish (n=16) was assessed for 40 minutes. In addition, three fish pairs of age 5–6 mpf containing both sexes from both IL groups ([DBNH][OAc] and $[P_{4441}]$[OAc]) were selected for breeding studies and for a histological examination, focusing on reproductive organs, liver, gills, and intestines. More information can be found in Paper I.

4.2.3. Cytotoxicity assays

CHO, HCE, and *E. coli* cells were grown to confluence at 37 °C. The mammalian cells were serum starved and treated with ILs for 20 to 24 hours with ILs, while *E. coli* cells were incubated with ILs for three hours. Redox sensitive alamarBlue dye, which is a fluorometric/colorimetric cell viability indicator, based on the detection of metabolic activity of cells,[113, 114] was added to the wells 1–2 hours before the incubation time expired. The alamarBlue reagent shifts from a non-fluorescent state (blue) to a fluorescent state (red) in the presence of intracellular reducing agents (live cells). The fluorescence (HCE, CHO) or absorption (*E. coli*) was measured using a plate reader. The number of viable cells in each well were determined from a calibration curve that was proportional to the fluorescence/absorption shift of the alamarBlue reagent. The EC_{50} values were determined from a logistic sigmoid function that was applied to the number of cells versus IL concentration graph. All

errors are given as standard deviations (SD). More information can be found in Papers I (CHO cells), II (HCE and *E. coli* cells), and V (HCE cells).

The bioluminescence of *V. fischeri* cells were determined using a Microtox instrument for at least four different IL concentrations in 2% (w/v) sodium chloride solution. The decay in the bioluminescence is proportional to the concentrations of a toxicant. The EC_{50} values were determined five and 15 minutes post IL treatment, following the instructions of the manufacturer. More information can be found in Papers IV and V.

HCE cells were used for the real-time cytotoxicity assay. Cells were treated with ILs (Paper V) at their EC_{50} concentrations. A cyanine dye, which stains the DNA strand of the dead cells once the integrity of the plasma membrane has been compromised, was added. Upon binding to DNA from non-viable cells, the dye becomes fluorescent, and the fluorescence is directly proportional to the level of cell death.[115] Changes in the fluorescence signal were measured 0.5, 2, 4, 8, and 24 hours post IL treatment. More information can be found in Paper V.

Human red blood cells were used for a hemolysis assay.[110] Collected blood was washed and diluted in phosphate buffer saline (PBS). The RBC cells were treated with ILs for approximately 20 minutes. The unbroken RBC pellets were removed and the absorbance of hemoglobin was measured from the supernatant. The relative hemolysis was determined by comparing the absorbance to the controls. More information can be found in Paper V.

4.2.4. Liposome preparations

Liposomes were prepared by mixing proper molar proportions of lipids in chloroform (Table 6) to yield a desired total concentration. Chloroform was evaporated to dryness under a stream of air and the residues were removed keeping the sample in a desiccator under reduced pressure for at least 16 hours. The lipid film was hydrated in a proper solvent (water; Papers IV and V or buffer; Papers II and III) by shaking the dispersion for 60 minutes at 60–70 °C. The resulting multilamellar vesicle dispersion was further processed to unilamellar vesicles by extruding the dispersion through a 100 nm pore size filter 19 times. DPPC aggregate and fuse already after one day[116] and therefore the DPPC liposomes (Papers IV, V) were not extruded, but used as MLVs. The sizes were routinely confirmed by DLS using a Zetasizer instrument.

Prior to extrusion the RBC lipids were extracted from intact RBCs following the Bligh-Dyer protocol[109] and the solvent was evaporated using nitrogen gas. More information can be found in Paper III. The RBC extracted lipids were prepared in the same manner as the synthetic lipids.

Table 6. Lipids and their mixing ratios used in liposome preparations.

Lipid mixture	Mixing ratio (mol%)	Paper
eggPC/POPG eggPC/POPG/Chol	75/25 50/25/25	II
POPC/POPG POPC/POPG/Chol RBC	80/20 60/20/20 100	III
DPPC	100	IV, V
eggPC/eggPG	80/20	V

4.2.5. Buffer preparation

Sodium phosphate buffer was prepared by mixing sodium hydrogen phosphate and sodium dihydrogen phosphate to yield a pH of 7.4 and an ionic strength (I_S) of 10 mM (Paper II) or 20 mM (Paper III). The buffer solution was filtered through a 0.45 µm syringe filter. The pH was confirmed with a pH meter and adjusted with a sodium hydroxide (NaOH) or a hydrogen chloride (HCl) solution, if it was needed.

4.3. Analysis conditions

4.3.1. Critical micelle concentration determinations

Two complementary techniques were used for the CMC determinations of the ILs. In contact angle meter measurements the ILs were diluted in ultrapure water to a final volume of 700 µl at various concentrations below and above their assumed CMC values. The surface tension is proportional to the drop shape,[117] therefore four drops of each IL concentration were formed and 20 frames were taken of each drop. An average of the surface tension of each concentration was calculated and plotted against increasing concentration of the IL. Finally, the CMC was derived from the intersection point where the surface tension reached a relatively constant value.

In CE studies, the ILs were diluted in water or in phosphate buffer (Papers I and II) at various concentrations. A fused silica capillary with an inner diameter of 50 µm and an outer diameter of 375 µm was used. The total capillary length was 47.0 cm and the length to the detector was 38.5 cm. New capillaries were preconditioned by pressure at approximately 950 mbar with 0.1 M NaOH for 10 min, with water for 10 min, and with the IL solution for two min. A constant voltage of 25 kV (corresponding to a field strength of 530 $V \cdot cm^{-1}$) was applied for 1.5 min and the current was recorded and plotted against an increasing concentration of the IL. Two linear trend lines were applied and the CMC was derived from the intersection point of the lines. The runs were repeated at least three times and the errors were reported as SDs.

4.3.2. Size and zeta potential determinations

All size and zeta potential measurements were done at 20 °C (Paper V) or at 25 °C (Paper II) employing a helium/neon laser at 633 nm. Liposome dispersions were diluted to a concentration of 0.05–0.15 mM to yield an optimal scattering intensity. Disposable cuvettes and disposable folded capillary cells were used for the size and zeta potential measurements, respectively. A constant voltage of 150 V was used (corresponding to a field strength of 30 $V \cdot cm^{-1}$). All measurements were conducted at least three times — one run consisting of minimum 10 individual measurements. The errors were reported as SDs. ILs were mixed with the liposomes 10–15 minutes before the measurements.

4.3.3. Capillary electrophoresis

CE with a diode array detector was used for the determination of the distribution constants of local anesthetics (Paper III). Wavelengths of 200, 214, 238, 254, and 280 nm were used. The total length of the uncoated fused silica capillary, with an inner diameter of 50 µm and an outer diameter of 375 µm, was 38.5 cm and the distance to the detector was 30.0 cm. A constant voltage of 20 kV (corresponding a field strength of 520 $V \cdot cm^{-1}$) was used throughout the study. Thiourea was used as an EOF marker and sodium phosphate buffer (pH=7.4, I_S=20 mM) was used as the BGE. New capillaries were preconditioned by rinsing at a pressure of ~950 mbar for 15 min with 0.1 M NaOH and for 15 min with water. In CE the preconditioning was followed by a rinse with sodium phosphate buffer for five min and in LEKC studies a 1–3 min rinse with the PSP. All runs were repeated at least five times and the errors were reported as SDs.

4.3.4. Differential scanning calorimetry

DSC was used for assessing the permeation of the ILs into the liposome membrane. DPPC liposomes were used due to their well-defined phase transition temperature at 41.3 °C.[118] DPPC liposomes, with varying concentrations of IL, were diluted in water yielding a final lipid concentration of 0.4 mM. Samples were degassed ca. five minutes prior to the DSC measurements to remove bubbles. A heating rate of 60 $°C \cdot h^{-1}$ was used within a temperature range of 10 to 60 °C (Paper V). Three heating and three cooling scans were recorded and the samples were kept at the lowest temperature for 30 minutes before the heating scans. The errors were reported as SDs.

4.3.5. Nuclear magnetic resonance spectroscopy

NMR was used in order to assess the diffusion of ILs with and without the presence of liposomes. In DOSY measurements the gradient strength (G) of the pulses varied between 2 and 95% of the maximum gradient strength of 0.47 $T \cdot m^{-1}$ in 32 steps. The durations of the gradient pulses (δ, 2 ms), the delay time (Δ, 150 ms), and the temperature (T, 21 ˚C) were kept constant. The gyromagnetic ratio (γ) was 42.6 $MHz \cdot T^{-1}$ for ^{1}H nuclei.

5. RESULTS AND DISCUSSION

5.1 Effect of ionic liquids on zebrafish

In order to evaluate the effect of ILs on living organisms and especially on different organs, zebrafish studies were performed. Phosphonium-based ILs having various cation and anion chain lengths were chosen to the study (Figure 5; Paper I). In addition, a long-term impact of two potential biomass dissolving ILs ([DBNH][OAc] and $[P_{4441}][OAc]$) were assessed.

5.1.1 Viability of larvae

The impact of cationic and anionic ILs on the viability of zebrafish embryos and larvae was assessed by growing the fish in IL solutions for five days (Figure 6). All measurements were repeated three times and the errors are given as standard error of means (SEM). Two concentrations of each IL classes were used (1 $mg \cdot L^{-1}$ and 100 $mg \cdot L^{-1}$ or 1 $mg \cdot L^{-1}$ and 10 $mg \cdot L^{-1}$). The lower concentration (10 $mg \cdot L^{-1}$) was used for the ILs having long anion chain lengths ($[P_{4441}][C_nH_{2n+1}COO]$; $n \geq 13$) due to precipitation in the media. Analysis of variance (ANOVA) was applied to the data to assess the significance of the results. Because the data had two independent variables (time and the IL treatment) and the data was normally distributed, two-way ANOVA with Dunnett's multiple comparison test was used based on recommendations for such data.[119, 120]

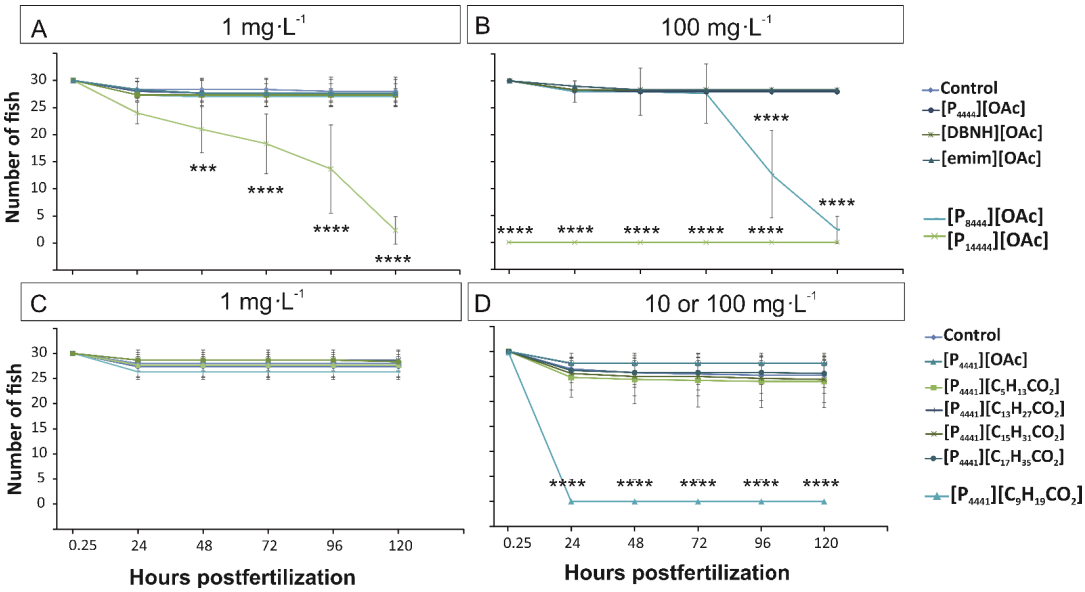

Figure 6. Viability of the zebrafish embryos. Two-way ANOVA with Dunnett's multiple comparison test. Time × treatment interaction, n=30 at initial time point. Results are presented as mean±SEM, ***p<0.001 and ****p<0.0001. Effect of A and B) cationic ILs C and D) anionic ILs on the zebrafish viability. Adapted with permission from "Ruokonen, S.-K., et al., 2016, Environ. Sci. Technol., 50, (13), 7116-7125." Copyright (2018) American Chemical Society.

100 mg·L^{-1} [P_{14444}][OAc] was lethal to all zebrafish embryos within 10 min, whereas 1 mg·L^{-1} showed time dependency and killed all the fish after 120 hours (5 days) post treatment (Figure 6B and A, respectively). [P_{4441}][OAc], [DBNH][OAc], and [emim][OAc] on the other hand, were not toxic at the tested concentrations (Figure 6A and B). Their EC_{50} values are >100 mg·L^{-1}, thus, they can be considered as practically harmless or harmless based on the GHS classification system.[112]

Zebrafish embryos hatch from their chorions on average on the third day postfertilization.[121] This leads to a direct exposure of the larvae to the environment and external toxicant. After 24 and 72-120 hours post treatment, 100 mg·L^{-1} of [P_{4441}][C_9H_{19}COO] and [P_{8444}][OAc], respectively, were lethal to the embryos (****p<0.0001; Figure 6B and D). [P_{4441}][C_9H_{19}COO] kills the embryos already within 24 hours, meaning that the IL penetrates into the embryo chorions. Therefore, [P_{4441}][C_9H_{19}COO] can be considered to be more toxic than [P_{8444}][OAc], which initializes larvae mortality after the larvae are hatched from their protecting chorions. However, the afore mentioned ILs were not toxic at all when embryos were treated with a 1 mg·L^{-1} concentration of the ILs.

The other anionic ILs, [P_{4441}][C_5H_{13}COO], -[$C_{13}H_{27}$COO], -[$C_{15}H_{31}$COO], and -[$C_{17}H_{35}$COO], did not have any significant effect on the viability of the zebrafish embryos and larvae during 5 dpf (Figure 6 C and D). This was probably due to the short chain of [P_{4441}][C_5H_{13}COO] and the low concentration

(10 mg·L^{-1}) of the long anionic ILs ([P_{4441}][$C_nH_{2n+1}COO$] n≥13) used. The results indicate that the EC_{50} values of the long anionic ILs were above 10 mg·L^{-1} and above 100 mg·L^{-1} for [P_{4441}][$C_5H_{13}COO$].

5.1.2 Ionic liquid-induced malformations on zebrafish larvae

The effect of ILs on the malformation of the fish phenotype was assessed by dividing all the 5 dpf fish into three groups based on their phenotypic malformations: no malformations, mild malformations, and severe malformations (Figures 7A, B, and C, respectively).

Figure 7. Zebrafish having A) no malformation, B) mild malformations, and C) severe malformations. Adapted with permission from "Ruokonen, S.-K., *et al.,* 2016, *Environ. Sci. Technol.,* 50, (13), 7116-7125." Copyright (2018) American Chemical Society.

The group exhibiting mild malformations had bent tail, short trunk, mild deformation in the head area, yolk sac edema, and pericardium edema, whereas the group with severe malformation had severely defective (short and curved) trunk development, truncated tail, small eyes, deformations in the head area, and yolk sac edema. The IL groups that were lethal to embryos on the viability tests (*i.e.,* 100 mg·L^{-1} of [P_{14444}][OAc] and 100 mg·L^{-1} of [P_{4441}][$C_9H_{19}COO$]) were not included in the study; only live fish could be used for the malformation assessment.

Long alkyl chained [P_{14444}][OAc] at 1 mg·L^{-1} and [P_{8444}][OAc] at 100 mg·L^{-1} caused mild malformation on the larvae (two-way ANOVA with Dunnett's multiple comparison test *$p<0.05$; n=10 and **$p<0.01$; n=7, respectively). 100 mg·L^{-1} of [P_{4441}][$C_5H_{11}COO$], which had the highest concentration of the anionic ILs, was the sole IL causing severe malformation on the zebrafish larvae (*$p<0.05$; n=120). [P_{14444}][OAc] and [P_{8444}][OAc] are the most hydrophobic cationic ILs tested. Thus, it was expected that these ILs penetrate the fish tissues and cause more damage than the anionic ILs. In order to assess the effect of the hydrophobic moiety location, tests were performed on these ILs using cells.

5.1.3 Long-term effect of ionic liquids on zebrafish

Two and a half months old fish, grown 5 days after fertilization in media with 100 $mg \cdot L^{-1}$ of [DBNH][OAc] or [P_{4441}][OAc], were chosen for further long-term studies due to their excellent biomass dissolving capability. The long-term tests consisted of assessing the behavior, breeding, and histology of the fish.

Due to an outcome of natural selection, different species exhibit several syndromes, which show as individual differences in behavior.[122] These differences reflect heritable, fundamentally different alternative strategies to cope with environmental changes. Aggressive individuals show an active response to external stimuli, whereas nonaggressive individuals adopt a passive strategy. Therefore, different external alterations may have an impact on the behavior of individuals.

Three behavior assays (locomotor activity, novel object, and aggressive-boldness assessment) were applied to the adult fish. The behavior of the IL treated fish were compared to the behavior of the control group but no significant changes were observed in the behavior of the fish, indicating that the ILs did not have major effects on the fish activities.

The effect of ILs on the fish spawning was tested using five to six months old fish. Three control fish groups were able to spawn in a controlled environment, producing 78, 94, and 103 embryos. The reason for the relatively small numbers of spawning couples can be the young age of the fish and lack of previous experience of spawning. [DBNH][OAc] treated fish did not spawn at all. [P_{4441}][OAc]-treated fish spawned once and produced 243 embryos, which is almost three times more than the average number produced by the control group. However, because only one pair spawned, it is plausible that the large number of embryos is not due to the effect of the IL. Because of the small amount of spawning couples, no statistical analysis could be performed and no solid conclusion could be drawn from the data. The produced embryos were grown for seven days and there were no significant differences between the control group and the [P_{4441}][OAc] treated larvae offspring.

Histological examinations was conducted for the six months old fish. The fish were sagittally sliced and stained with hematoxylin and eosin dye. The histological differences between the control group and the [DBNH][OAc] and [P_{4441}][OAc] treated fish were compared using a light microscope focusing on liver, gills, intestines, and especially on gonads. However, no significant differences were observed.

[DBNH][OAc] and [P_{4441}][OAc] did not cause any significant impact on the behavior, breeding, nor histology of the adult zebrafish, and therefore these ILs can be considered relatively safe to fish at the used concentrations.

5.2 Interactions of ionic liquids and cells

5.2.1 Determination of median effective concentration

In order to evaluate the toxicity of ILs, various cells lines were utilized. First, a set of ILs (Paper II, Figure 5; 0.1–1000 mg·L^{-1}) were chosen for cytotoxicity testing using HCE and *E. coli* cells. Because the same IL concentration range was used for all ILs, only the long alkyl chained phosphonium ILs, [P_{14444}][OAc], [P_{14444}]Cl, [P_{8444}][OAc], and [P_{8444}]Cl could exert toxicity. Next, CHO, HCE, and *V. fischeri* cells were utilized for assessing the selection of cell line (Figure 8A), the effect of cation chain length (Figure 8B), and the effect of anion chain length (Figure 8C) on the IL cytotoxicity (Papers I and V).

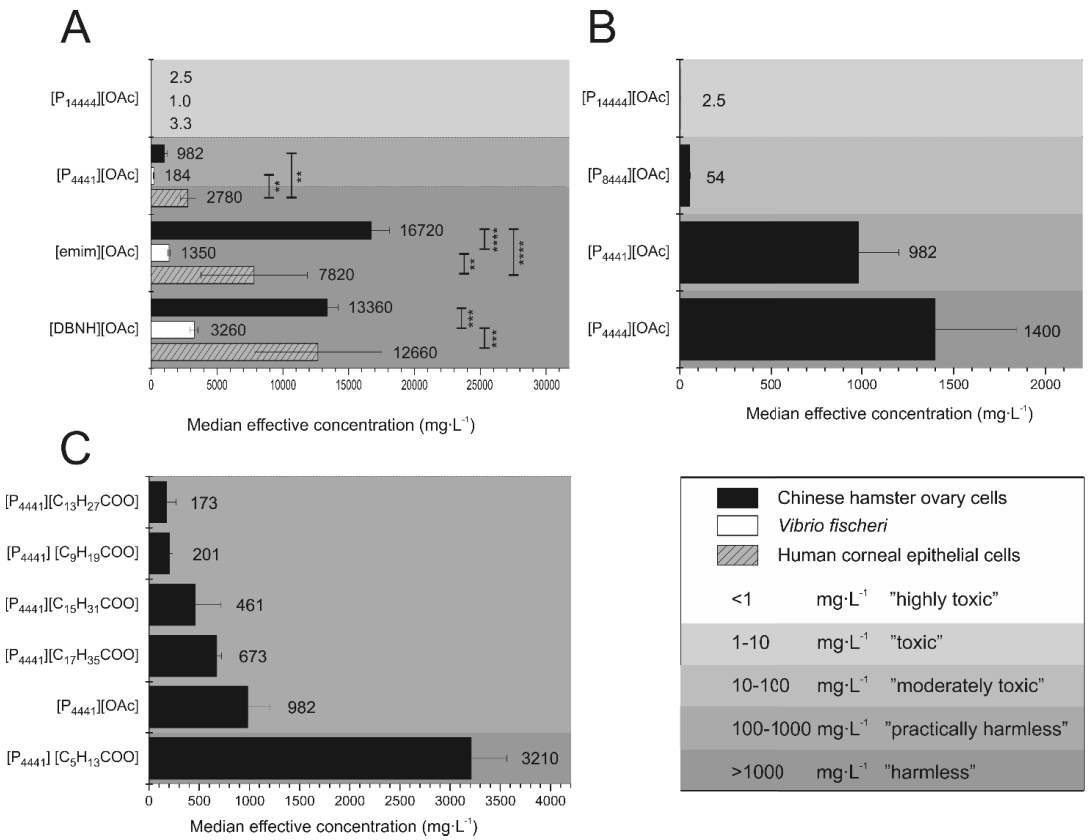

Figure 8. EC_{50} values of various ILs. Impact of A) selected cell line, B) cation chain length, and C) anion chain length.

All ILs were more toxic toward the bacteria (*V. fischeri*) than toward the mammalian cells (CHO, HCE; Figure 8A). The difference was significant (one-way ANOVA with Tukey HSD post-hoc test) in the case of $[P_{4441}][OAc]$, [emim][OAc], and [DBNH][OAc]. Similar difference in the cytotoxicity values between bacterial and mammalian cells have been shown before for ILs[41] and energetic compounds (such as 2,4,6-trinitrotoluene and 1,3,5-trinitrobenzene).[123] HCE cells were incubated with the ILs for 24 hours instead of 15 minutes that was used for *V. fischeri cells,* indicating that the mammalian cells were more resistant than the bacterial cells toward the ILs. Different organisms are known to have different susceptibilities to xenobiotics[42, 124-126] and the difference can be due the variation in the cell structure and metabolism of the prokaryotic and eukaryotic cells. Another plausible explanation is the difference in the EC_{50} determination methods of the assays. Whereas the redox sensitive alamarBlue dye is proportional to the alive to dead cell ratio, the decay in the bioluminescence of the *V. fischeri* bacteria is recorded. It is plausible that a same concentration of IL that causes bioluminescence quenching would not be enough to kill the cells, hence, the median lethal concentration (LC_{50}) for the ILs using the *V. fischeri* cells could be bigger than the EC_{50} values obtained here.

Figure 8B shows that elongation of the cation chain length increases the cytotoxicity (decreases the EC_{50} value). The correlation of cytotoxicity and lipophilicity has been shown several times before[63, 127] and it is speculated that the lipophilicity of the cation is the dominating factor for ionic liquid toxicity.[12, 128] Moreover, the size of the cation has been shown to affect more on the toxicity than the three-dimensional shape of the cation.[129]

It has been shown, that the cytotoxicity does not increase linearly with lipophilicity for highly lipophilic compounds — the cytotoxicity becomes relatively stable after a certain “cut-off alkyl chain length”. For example Pernak *et al*.[130] have shown that the cut-off alkyl chain length would be 12 carbons and Ranke *et al.* that compounds having a chain length of 12–14 carbons in benzoalkonium chlorides have similar cut-off effects.[12] The cut-off effect is also shown to be dependent on the type of organism. Ventura *et al.* showed that the effect could only be seen using *Staphylococcus aureus* bacteria, but it was not be observed with *Esterichia coli* bacteria, *Fusarium sp*. fungus, nor *Candida albicans* yeast.[131] It has been speculated that this effect could occur due to insufficient solubility of the compound in the media. Other plausible explanation is the change in the kinetics of the compounds upon increased molecular mass (*e.g.* cellular uptake slows down in the case of large molecules).[18]

Even though the effect of cation chain length is under discussion in a myriad of studies, the effect of anion chain length has gained less attention. Petkovic *et al*.[132] showed that the toxicity (minimal inhibitory concentration, MIC) increased upon an increase of the anion chain length of cholinium carboxylate (C2–C10) ILs using filamentous fungi. Rengstl *et al*., on the other hand, showed that the

cytotoxicity (HeLa and SL-MEL28 cells) increased for cholinium carboxylates when the anion chain length varied between 6 to 10, while the toxicity was not linear in the range of C2 to C5. Santos *et al*. got similar results — the toxicity increased when the anion chain length of cholinium carboxylate ILs were elongated from 2 to 5 carbons using *Daphnia magna* crustacean, however there was no clear trend in the toxicity when microalgae, macrophytes, or bacteria were used.[133] Furthermore, Muhammad *et al*. showed that the elongation of the cholinium carboxylate anions from 2 to 6 actually decreased the cytotoxicity instead of increasing it[134] and Weyhing-Zerrer *et al*. showed that the elongation of imidazolium based cations (C2-C6) decreased the IL toxicity when bulky tris(pentafluoroethyl)trifluorophosphate (FAP) anion were used.[135]

It seems that the elongation of the anion moiety increases the toxicity only when a certain "threshold carbon amount", usually C>6, is exceeded. This indicates that the toxicity does not always increase linearly when the anion chain length is increased. It is plausible that this is characteristic only for IL anions, however, a similar effect was also observed for $[P_{4441}][OAc]$ and $[P_{4444}][OAc]$ (EC_{50} values 982 and 1400 $mg \cdot L^{-1}$, respectively).

Hartmann *et al*.[136] showed that the elongation of carboxylate anions from 2 to 10 carbons indeed promoted the toxicity of the ILs but that they were unable to induce fungal plasma membrane damage, even at concentrations leading to cell death. It was speculated that the impact might occur due to electrostatic repulsion between the negatively charged IL moiety and the negatively charged plasma membrane.

The increase of toxicity upon elongation of the anion chain length was not as strong as in the case of the cation (Figure 8B and C). Elongation of the acetate anion of $[P_{4441}][OAc]$ to 14 carbons ($[P_{4441}][C_{13}H_{27}COO]$), decreased the EC_{50} value 6 fold (increased the toxicity). However, the decrease in the EC_{50} value was 393 fold when the cation chain length was elongated by the same amount of carbons from $[P_{4441}][OAc]$ to $[P_{14444}][OAc]$. This indicated that $[P_{4441}][C_{13}H_{27}COO]$ was approximately 70 times less toxic than $[P_{14444}][OAc]$. Sosnowska *et al*.[129] have shown that elongation of the anion increases the toxicity of the ILs, yet the anion effect never exceeds the effect of a cation. Interestingly the toxicity decreased when the acetate anion was changed to hexanoate. It is plausible that in the case of $[P_{4441}][OAc]$ the cation determines the toxicity and when the anion chain length is increased to hexanoate the anion interacts with the membrane, slightly preventing the interaction between the cation and the plasma membrane. It seems that the toxicity increased when the anion chain length exceeded 10 carbons. However, the increment was not gradual. In order to assess whether the aggregation behavior of the ILs affect their cytotoxicity, the EC_{50} values were compared with the CMC values.

5.2.2 Effect of ionic liquid aggregation on toxicity

Surface-active compounds aggregate when their concentrations exceed their critical micelle (or aggregation) concentrations. The CMCs were measured using two techniques: CAM (Papers I, IV, V) and CE (Papers I and II). Comparison of the obtained CMCs are shown in Figure 9.

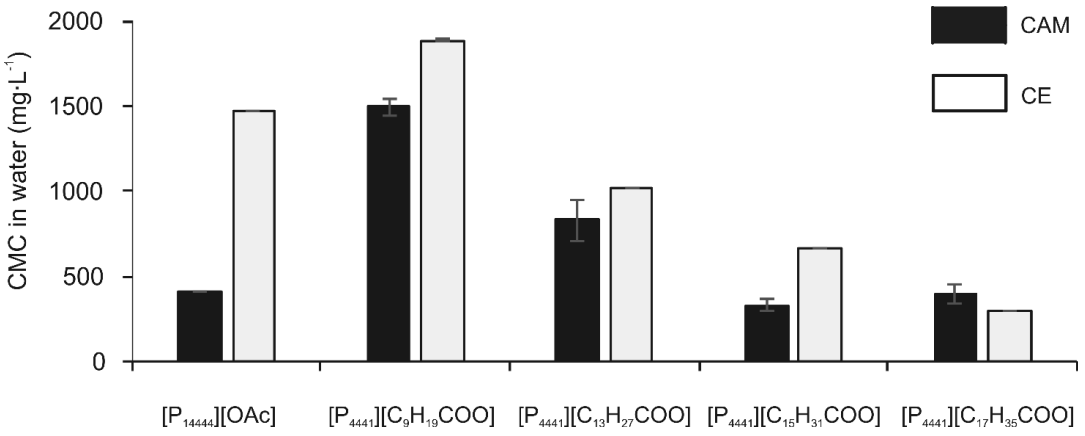

Figure 9. CMC values of phosphonium-based ILs obtained using CAM and CE.

The CMC values obtained using both methods varied slightly. In capillary electrophoresis, the CMC is obtained by measuring the electric current, which is linearly dependent on the conductivity of the electrolyte solution at constant voltage. The current increases linearly upon increased surfactant concentration. The increase in the current slows down when the mobility of the surfactant becomes slower once the surfactants are occurring in an aggregated form instead of occurring as single unimers.[137-139] Thus, the CMC can be derived from the intersection point of two linear trend lines applied to the current versus IL concentration graph.

In CAM, the CMC is determined by plotting the surface tension as a function of increasing IL concentration and deriving the intersection point where the surface tension is not changed remarkably upon addition of unimers. At this point, a balance between unimers, oriented at the surface of the drop, and the aggregates is formed and all additional unimers aggregate and the surface tension stays relatively constant.[104]

All the CMC values were smaller using CAM than when CE was used, except $[P_{4441}][C_{17}H_{35}COO]$. This can be explained by the difference between the methods. The change in the current in CE caused by IL aggregation is hardly distinguishable, especially for ILs that aggregate gradually *i.e.,*

the aggregation occurs slowly in a broad concentration range. The change in the surface tension was more prominent and therefore the optical pendant drop method was more trustworthy and preferred.

The effect of IL aggregation on the cytotoxicity of ILs is shown in Figure 10 (Paper I and IV).

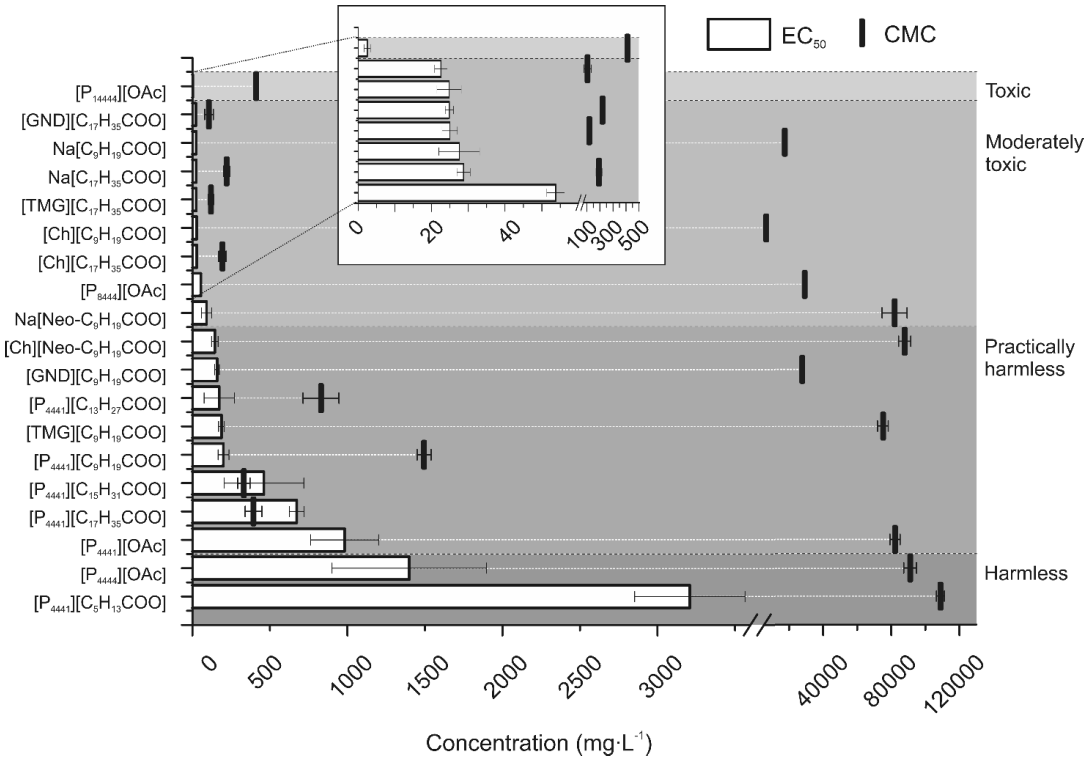

Figure 10. Cytotoxicity of ILs using CHO cells and the CMC values of the ILs.

Most of the CMCs were remarkably above the EC_{50} values, indicating that the ILs were interacting with the cells as free unimers. However, $[P_{4441}][C_{15}H_{31}COO]$ and $[P_{4441}][C_{17}H_{35}COO]$ ILs having long alkyl chain lengths in the anion moiety were aggregating or more likely reached their solubility limits before reaching their EC_{50} values. Most surface-active compounds have specific Krafft points (*i.e.,* Krafft temperatures). Surfactants are not able to attain their CMCs below this temperature because their solubility limit is reached and they precipitate out of the solution.[140] Because of this precipitation there were no free unimers in the solution and hence the toxic phenomenona excerted by $[P_{4441}][C_{15}H_{31}COO]$ and $[P_{4441}][C_{17}H_{35}COO]$ were weaker than the effect caused by the other similar anionic ILs ($[P_{4441}][C_9H_{19}COO]$ and $[P_{4441}][C_{13}H_{27}COO]$). This explains why the cytotoxicity does not increase linearly when the alkyl chain length of the anion moiety is elongated from 2 ($[P_{4441}][OAc]$) to 18 ($[P_{4441}][C_{17}H_{35}COO]$).

5.2.3 Time-dependent cytotoxicity

The EC_{50} measurements showed that the ILs exert toxicity over a wide range of concentrations (Figures 8 and 10). Figure 11 shows results of a CellTox™ assay, which was used to determine the time of appearance of the cell mortality after treatment with ILs (Figure 5; Paper V) at their EC_{50} values. Thus, the expected maximum mortality was expected to be 50%.

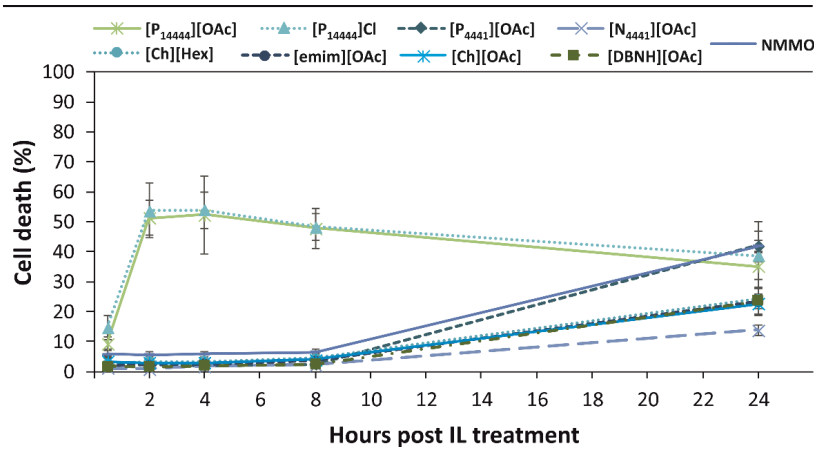

Figure 11. Real-time measurement of the cytotoxicity of ILs. HCE cells were treated with the compounds at the following concentrations: 4 mg·L^{-1} [P_{14444}][OAc], 3 mg·L^{-1} [P_{14444}]Cl, 3300 mg·L^{-1} [P_{4441}][OAc], 7800 mg·L^{-1} [emim][OAc], 11 800 mg·L^{-1} [Ch][OAc], 3300 mg·L^{-1} [Ch][Hex], 3100 mg·L^{-1} [N_{4441}][OAc], 12 900 mg·L^{-1} [DBNH][OAc], and 31 600 mg·L^{-1} NMMO. Data was collected at 2, 4, 8, and 24 hours post treatment. Adapted with permission from "Ruokonen, S.-K., *et al.*, 2017*, Chem.-Eur. J.,* 2018, 24, (11), 2669–2680." Copyright (2018) John Wiley & Sons, Inc.

Most of the ILs ([P_{4441}][OAc, [N_{4441}][OAc], [Ch][Hex], [emim][OAc], [Ch][OAc], [DBNH][OAc], and NMMO) behaved in a similar manner, exerting cytotoxicity after a lag period of 8 hours. Noticeable exceptions were the long chained phosphonium ILs, [P_{14444}]Cl and [P_{14444}][OAc], which reached their maximum toxicity levels in less than 2 hours of incubation. The CellTox™ assay utilizes a non-permeant fluorescent cyanide dye that highlights cell breakage by interacting with the DNA of a ruptured cell.[115, 141] Thus, the results suggest that [P_{14444}]Cl and [P_{14444}][OAc] are the most efficient ILs at destabilizing the plasma membrane and they affect significantly the integrity of the cellular membrane by lysing the cells.

[N_{4441}][OAc], [Ch][Hex], [emim][OAc], [Ch][OAc], and [DBNH][OAc] could not induce 50% cell death, even though the cells were treated with their EC_{50} concentrations (obtained using HCE cells; Paper

V). This can be because the assay for the determination of the EC_{50} values and the real-time cytotoxicity assay employ different methods of detection. Instead of highlighting cell rupturing (CellTox^{TM}), the alamarBlue uses a membrane permeable dye and highlights the metabolic activity. This indicates that the mechanism of toxicity for $[N_{4441}][OAc]$, [Ch][Hex], [emim][OAc], [Ch][OAc], and [DBNH][OAc] is not related to membrane alteration but these ILs more likely interact with the cells by other means. For example, $[N_{4441}][OAc]$ at its EC_{50} concentration kills 50% of the HCE cells by affecting the metabolism whereas the cell death is only 15% in the real-time cytotoxicity assay after 24 hours. This indicates that the plasma membrane integrity is not significantly altered. On the other hand, for $[P_{4441}][OAc]$ a similar concentration affects equally the metabolism and the permeability of the plasma membrane. Using both methods, we obtained information about the cytotoxicity of ILs from different perspectives.

5.2.4. Hemolysis

A hemolysis assay was used to determine whether the mechanism of toxicity is related to membrane brakeage or not. RBC cells were treated with ILs (Figure 5; Paper V) at concentrations below and above their EC_{50} concentrations, for approximately 20 minutes. The results are shown in Figure 12.

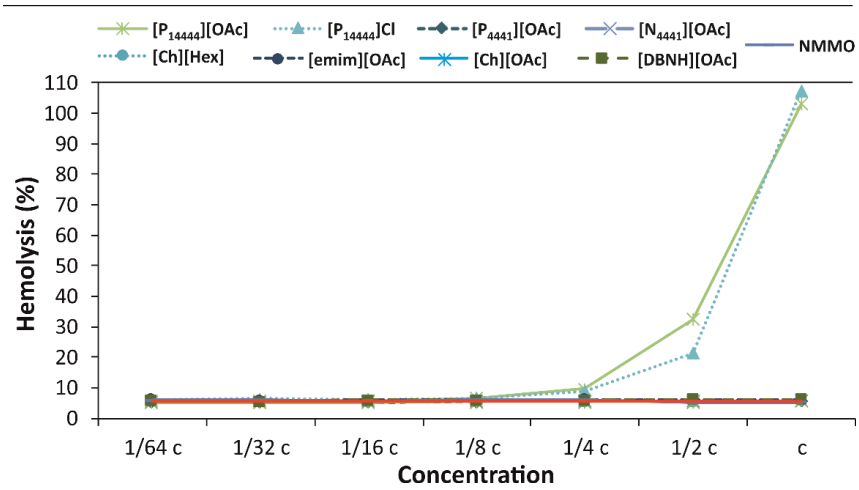

Figure 12. Hemolysis of red blood cells. Hemolysis was assessed using binary dilutions. Initial concentrations (c) were as follows: 20 mg·L^{-1} $[P_{14444}][OAc]$, 20 mg·L^{-1} $[P_{14444}]Cl$, 12400 mg·L^{-1} $[P_{4441}][OAc]$, 25 000 mg·L^{-1} [emim][OAc], 49 900 mg·L^{-1} [Ch][OAc], 50 000 mg·L^{-1} [Ch][Hex], 12 500 mg·L^{-1} $[N_{4441}][OAc]$, 49 900 mg·L^{-1} [DBNH][OAc], and 99 600 mg·L^{-1} NMMO. The red line indicates the negative control level of hemolysis. Adapted with permission from "Ruokonen, S.-K., *et al.,* 2018, *Chem.-Eur. J.,* 2018, 24, (11), 2669–2680." Copyright (2018) John Wiley & Sons, Inc.

Only $[P_{14444}][OAc]$ and $[P_{14444}]Cl$ were able to lyse the RBCs within 20 minutes and the lysis occurred at IL a concentration (5 $mg \cdot L^{-1}$) where the EC_{50} value was exceeded (3.3 $mg \cdot L^{-1}$ for $[P_{14444}][OAc]$ and 1.8 $mg \cdot L^{-1}$ for $[P_{14444}]Cl$; Paper V). These ILs exert toxicity intercellularly affecting the cell integrity. First, the other tested ILs, including $[P_{4441}][OAc]$ and NMMO, which reached the 50% cell mortality in the real-time cytotoxicity test, could not lyse the cells within 20 minutes. This indicates that these compounds affect the metabolism of cells intracellularly or the membrane penetration requires more time and the short test period was only enough for cell lysis of the most lipophilic compounds ($[P_{14444}][OAc]$ and $[P_{14444}]Cl$). Secondly, no lysis occurred when the cells were treated with ILs ($[P_{4441}][OAc$, $[N_{4441}][OAc]$, [Ch][Hex], [emim][OAc], [Ch][OAc], [DBNH][OAc], and NMMO) at concentrations 3.1–15.2 times higher than the EC_{50} values. This suggests that the membrane interactions are not solely proportional to the IL concentration but the time to induce cell breakage plays a major role for ILs that are only moderately lipophilic, such as $[P_{4441}][OAc]$.

The hemolysis assay provided an insight into the mechanism of IL toxicity, however in order to gain more subtle information on the interactions between ILs and cell membranes, liposomes were used as biomimicking membranes.

5.3 Interactions between compounds and liposomes

The plasma membrane is the first cellular constituent encountered by an external toxicant when interacting with cells. Therefore, biomimicking liposomes are excellent models for assessing IL-membrane interactions. The concentrations of the studied lipids were selected based on two criteria: to correspond to those of the studied cells and to be suitable for the particular measurements. For example 0.15 mM of eggPC/eggPG (80/20 mol%) liposomes and 0.4 mM DPPC liposomes are equivalent to 295 and 565 billion liposomes, respectively, while the concentration of lipids in HCE cells was approximated to be 0.34 mM corresponding to 340 000 cells (Paper V).

5.3.1 Selection of liposome composition

The knowledge of the ability of a drug to interact with cell membranes is of importance when assessing the behavior of a drug in a biological environment. Understanding the hydrophobicity of a compound helps to predict and exploit the behavior in a wide range of situations, such as predicting drug solubility, drug delivery and interactions in the body, biological activity, transportation, distribution and accumulation of pollutants in the environment.[142] Moreover, the knowledge of the

partitioning and/or distribution of a drug between an aqueous phase and a hydrophobic phase, provides information on the hydrophobic (*e.g.* liposome) phase used.

Local anesthetics serve as good model compounds to study the distribution of drugs between different liposome phases, because they are fairly lipophilic and there are many studies regarding their physicochemical behavior.[143, 144] Three different liposomes compositions (80/20 mol% POPC/POPG, 60/20/20 mol% POPC/POPG/Chol, and 100% RBC liposomes) were assessed in order to find the most suitable model liposome for the further IL-liposome interaction studies. The effect of liposome lipid composition and temperature in the distribution constants of the local anesthetics are shown in Figure 13.

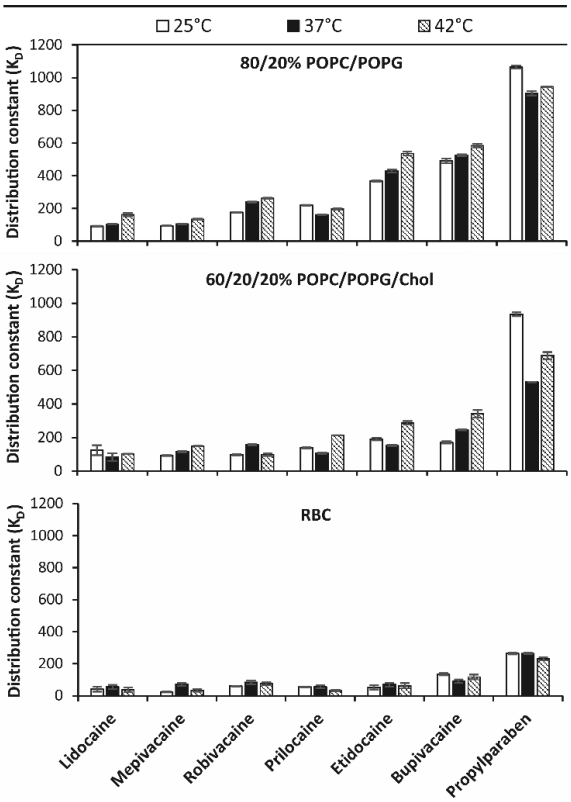

Figure 13. Effect of liposome composition and temperature on the distribution constants of analytes using 80/20 mol% POPC/POPG, 60/20/20 mol% POPC/POPG/Chol, and RBC liposomes as pseudostationary phases in LEKC. The BGE comprised 1 mM liposomes in sodium phosphate buffer at pH 7.4 (I_S=20 mM). Separation conditions are given in the experimental. Reprinted with permission from "Ruokonen, S.-K., *et al.* 2017, *J. Chromatogr. A,* 1479, 194-203." Copyright (2018) Elsevier.

All studied compounds had the strongest interactions with POPC/POPG liposomes. Negatively charged propylparaben (degree of ionization 12.9%) had the strongest interaction with all liposomes (POPC/POPG, POPC/POPG/Chol, and RBCs) at all temperatures. The high K_D of propylparaben suggests that it is readily lipophilic and introduction of the compound to a physiological environment leads to interactions with different lipophilic phases. This observation is in good agreement with previous studies where propylparaben has been shown to be absorbed

from the blood circulation and from the gastrointestinal tract to a variety of tissues.[145] In addition to propylparaben, bupivacaine and etidocaine had the strongest interactions with the liposomes, which is in a good agreement with the fact that they have the highest theoretical distribution constants (logD values).

Intercalating 20 mol% of cholesterol into POPC/POPG liposomes decreased the K_D values slightly and the decrease was highly dependent on the compound type. The hydroxyl group of cholesterol is positioned close to the polar head groups of the phospholipids maintaining the integrity of the cell wall and making the lipid bilayer more rigid, thus the passive permeability of the bilayer to small molecules is reduced.[75-80, 146] The most lipophilic anesthetics (bupivacaine and etidocaine) were affected more by the cholesterol addition than the less lipophilic anesthetics. However, this sort of correlation was not found in our previous study where common wastewater compounds were used.[147] Cholesterol is commonly known to diminish the retention of compounds into the liposomes. However, surprisingly it has also been shown to increase the interactions slightly when low concentrations of cholesterol (10–20%) were added into the POPC/POPS bilayer.[148] In addition, when the concentration of cholesterol were further increased, the interactions diminished.[149, 150] This suggests, that the compound structure has a major effect on how much the cholesterol addition to the liposome prevents compound-liposome interactions.

The K_D values of the compounds decreased approximately three fold when RBC liposomes were used as a pseudostationary phase. This can be due to the greater amount of cholesterol in the RBC liposome bilayer (49 mol%) than in the POPC/POPG (0%) and POPC/POPG/Chol liposomes (20%). Cholesterol is assumed to diminish the interactions of compounds and liposome bilayer causing a steric hindrance. Another plausible explanation is that the RBC liposomes contain less (8.5 mol%) negatively charged lipids (PS and PI) than the POPC/POPG liposomes (20%) and therefore the electrostatic interactions between the positively charged compounds (all except propylparaben) and the negatively charged liposomes are weaker.

Even though the RBC liposomes mimic real cell membranes the best, all studied compounds had stronger interactions with the PC/PG liposomes and therefore they were used in further studies to model cell membranes.

5.3.2 Effect of ionic liquids on liposome size and surface charge

Zetasizer was used for assessing the effect of ILs on the size and zeta potential of liposomes. First the impact of $[P_{14444}][AOC]$, $[P_{14444}]Cl$, $[P_{8444}][OAc]$, and [emim][OAc] on eggPC/POPG (75/25 mol% and eggPC/POPG/Chol 50/25/25 mol%) liposomes with and without cholesterol at concentrations 0,

0.1, 1, 10, 100, and 1000 mg·L^{-1} were assessed (Paper II). [P_{14444}][OAc] and [P_{14444}]Cl changed the zeta potential of the liposomes from negative to positive at concentrations between 10–100 mg·L^{-1} and ruptured the membrane at a concentration of 1000 mg·L^{-1}. [P_{8444}][OAc], on the other hand, diminished the zeta potential close to zero at a concentration of 1000 mg·L^{-1} and did not have any significant effect on the liposome size. [emim][OAc] did not have any effect on the liposome size nor zeta potential at tested concentrations. Addition of cholesterol did not have any remarkable effect on the IL interactions, even though cholesterol is known to diminish the interactions between compounds and membranes (*cf.* discussion above). One plausible explanation for this is that because [P_{14444}][OAc] and [P_{14444}]Cl had remarkable interactions with the liposomes at the concentration range used, the effect of cholesterol was too weak to be detected using the zeta potential and size measurements. Because only a narrow concentration range was used, more extensive studies were conducted using nine different ILs.

The effect of the nine ILs (Figure 5; Paper V) on eggPC/eggPG (80/20 mol%) liposomes was assessed below and above their EC_{50} values and the results are shown in Figure 14.

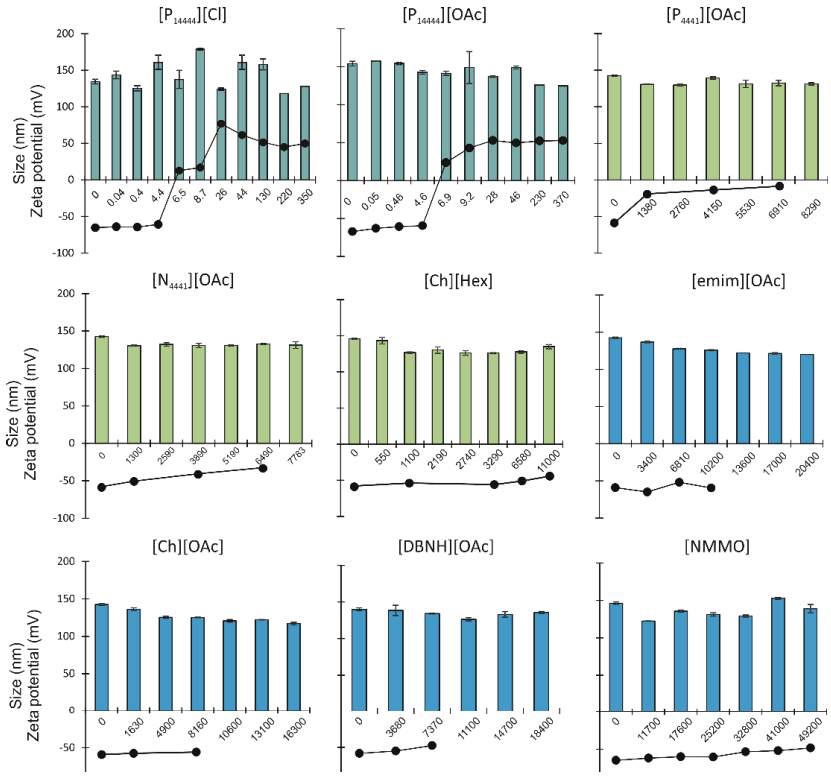

Figure 14. Effect of ILs and NMMO on the sizes (bars) and zeta potentials (dots) of 0.15 mM eggPC/eggPG (80/20 mol%) liposomes. Adapted with permission from "Ruokonen, S.-K., *et al*., 2018, *Chem.-Eur. J.,* 2018, 24, (11), 2669–2680." Copyright (2018) John Wiley & Sons, Inc.

The sizes of the liposomes did not change remarkably when ILs were added to the dispersions. However, the size distribution was more unstable when $[P_{14444}][OAc]$ and $[P_{14444}]Cl$ ILs were added to the dispersion compared to the other ILs. In addition, when the IL concentration exceeded 370 $mg \cdot L^{-1}$ (0.8 mM) the lipid bilayer was ruptured, and multiple sized aggregates could be detected. It can be seen from the zeta potential data that the $[P_{14444}]^+$ ILs permeate the lipid bilayer already at concentrations of 4.4–6.9 $mg \cdot L^{-1}$ (0.01–0.015 mM), converting the zeta potential of the liposomes from negative to positive. The concentrations causing a change are relatively close to their EC_{50} values, confirming that the mechanism of toxicity of $[P_{14444}]^+$ ILs is related to biomembrane permeation. $[P_{4441}][OAc]$ and $[N_{4441}][OAc]$, on the other hand, lowered the zeta potential close to zero but did not convert it to a positive. It seems that the ILs are loosely adsorbed on the liposome surface, diminishing the negative charge of the phosphate group, yet not covering it totally. The effect of [emim][OAc], [Ch][OAc], and [DBNH][OAc] ILs on the zeta potential of the liposomes could not be determined at concentrations near and above their EC_{50} values due to high conductivity and, thus, oxidation of the electrodes. However, it seems that the zeta potential did not change significantly at concentrations below the EC_{50} values. In addition, [Ch][Hex] and NMMO did not cause any significant changes to the liposome sizes nor the zeta potentials.

5.3.3 Effect of ILs on the liposome phase transition temperature

When a lipid bilayer is perturbed by an external surface-active compound, the lipid disorder increases, resulting in a decrease in the transition temperature (T_M) of the bilayer. This decrease in T_M was followed in order to assess the interaction between the ILs and the liposome bilayer, as shown previously.[11, 151] The results (Paper V) are presented in Figure 15.

The T_M did not change when [Ch][OAc], [DBNH][OAc], NMMO, and [emim][OAc] at concentrations six times higher than the EC_{50} values were introduced to the liposome dispersion. This indicates that the compounds did not compromise the order of the lipids and the mechanism of toxicity of these ILs is related to the alteration of the metabolism of the cells.

The phosphonium-based ILs $[P_{14444}][OAc]$, $[P_{14444}]Cl$, $[P_{4441}][OAc]$, and [Ch][Hex] decreased the T_M of the lipid bilayer at concentrations close to their EC_{50} values. This indicates permeation of the hydrophobic moiety of the IL into the membrane. This confirms the results from the real-time

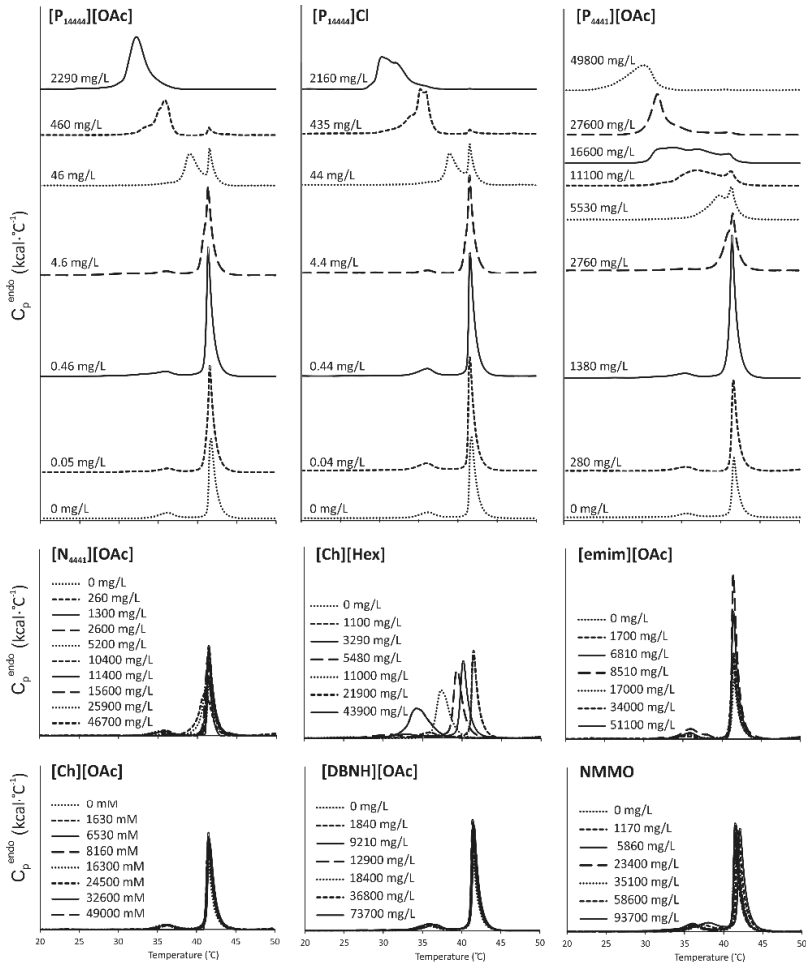

Figure 15. *Effect of ILs and NMMO on the phase transition temperature of 0.4 mM DPPC liposomes.* Adapted with permission from "Ruokonen, S.-K., *et al.,* 2018, *Chem.-Eur. J.,* 2018, 24, (11), 2669–2680." Copyright (2018) John Wiley & Sons, Inc.

cytotoxicity assay, hemolysis assays, and the zeta potential measurements, that the long alkyl chained ILs ([P_{14444}][OAc], [P_{14444}]Cl) interact with the cell membranes inducing toxicity.

A shift was observed in the endotherms for [P_{14444}][OAc] and [P_{14444}]Cl at a concentration range of 0.04–0.46 mg·L^{-1} (EC_{50} are 3.3 mg·L^{-1} and 1.8 mg·L^{-1} respectively, Paper V, HCE cells), for [P_{4441}][OAc] at 1380–2760 mg·L^{-1} (EC_{50} is 2780 mg·L^{-1}), and for [Ch][Hex] at 1100–3290 mg·L^{-1} (EC_{50} is 3420 mg·L^{-1}). Even though [Ch][Hex] affects the bilayer order, it only caused 25% cell rupture after 24 h incubation with the HCE cells (section 5.2.3., time-dependent cytotoxicity assay). It seems that in addition to the penetration of the IL into the bilayer compromising the integrity of the plasma

membrane, the toxicity of [Ch][Hex] is caused by an altered organism metabolism. [N_{4441}][OAc] did adsorb on the surface of the liposome, as seen from the zeta potential measurements, however, it did not permeate into the bilayer at its EC_{50} concentration lowering its T_M. The concentration of the IL causing the shift in the endotherm was approximately 10 times higher than the EC_{50} value, suggesting that the mechanism of toxicity of [N_{4441}][OAc] is related to an alteration in the metabolic activity of the cell and not to the penetration of the IL into the plasma membrane. This suggests that DSC is applicable to predict the concentration ranges where ILs, having surface-active properties, exert toxicity.

An increase in the concentration decreased the T_M gradually and another endothermic peak appeared in the thermogram when the phosphonium-based ILs [P_{14444}][OAc], [P_{14444}]Cl, and [P_{4441}][OAc] were added to the liposome dispersion. It has been shown before with surfactant-lipid mixtures that surfactants permeate the liposome bilayer saturating the liposomes with surfactant unimers.[47, 49] When the surfactant concentration is increased above the saturation concentration, the liposomes rupture and mixed lipid-surfactant micelles coexist with the mixed vesicles. The vesicle rupturing continues until a solvation concentration is reached where only mixed micelles appear. The two endotherms in the thermograms of [P_{14444}][OAc], [P_{14444}]Cl, and [P_{4441}][OAc] suggest this sort of a coexistence of vesicles with different amount of IL unimers in them (vesicles containing more surfactant unimers have lower T_M values). When the surfactant concentration is further increased only a small amount of IL saturated vesicles exist before the liposome rupture totally and no transition can be observed. Also, because we used MLVs in the DSC studies instead of unilamellar vesicles, it is also plausible that the heterogeneous outermost bilayer gives the signal at lower phase transition and the remains of the original signal at 41.3 °C is caused by the unaffected lipid lamellae close to the core of the liposome.

Usually the phase transition of pure liposomes is fast resulting in sharp peaks. This is due to cooperativity of the lipids, where conformational change in a molecule causes the adjacent molecules to adapt due to the high ordering of the lipid bilayer.[101] The peak areas decreased upon addition of the surface-active IL proving that the number of bilayers undergoing phase transitions is gradually decreasing. In addition of getting smaller, the endothermic peaks were wider when the lipid bilayer was perturbed with the surface-active ILs indicating a decrease in the lipid cooperativity.

5.3.4 Diffusion of ionic liquids

Compounds diffuse spontaneously in solution and the diffusion rate is dependent on the compound size. Thus, following the diffusion constants of ILs at different concentrations, with and without the presence of liposomes provide us information on the aggregation and location of the compounds.

The diffusion constants of $[P_{4441}][OAc]$, [emim][OAc], [Ch][OAc], [Ch][Hex], $[N_{4441}][OAc]$, [DBNH][OAc], and NMMO without liposomes did not change below and above the EC_{50} values, indicating that there were no aggregation of the compound unimers at the concentrations used (CMCs of the compounds are shown in Paper V). In addition, the diffusion constants of the aforementioned IL cations and anions did not change remarkably in the presence of liposomes, shown in Table 7.

Table 7. Diffusion constants of NMMO and IL cations and anions in the presence of eggPC/eggPG (80/20 mol%) liposomes.

	Concentration range ($mg \cdot L^{-1}$)	D_{Cation} (10^{-10} $m^2 \cdot s^{-1}$)	D_{Anion} (10^{-10} $m^2 \cdot s^{-1}$)
NMMO	590–58600	4.7–5.2	
$[P_{14444}][OAc]$	230–2300	0.1–0.6	5.8–7.1
$[P_{14444}][Cl]$	220–2200	0.1–0.6	5.8–7.1
$[P_{4441}][OAc]$	280–8300	3.5–3.6	6.5–6.7
$[N_{4441}][Oac]$	780–10400	3.4–3.7	6.5–6.8
[Ch][Hex]	220–11000	6.2–6.4	4.5–4.8
[emim][OAc]	170–12000	6.2–6.3	6.6–6.9
[Ch][OAc]	490–24500	6.2–6.5	6.5–6.9
[DBNH][OAc]	180–36800	5.2–5.5	6.2–6.6

Because the maximum concentrations used in this study were 1.5–200 times higher than the EC_{50} values of the ILs, we can assume that the possible IL-membrane interactions should be observable in this study. However, because the diffusion constants of the ILs were relatively similar with and without the liposomes it is likely that ILs are not tightly adsorbed nor absorbed onto/into the liposomes, but interact with cells either by binding to membrane receptors or by being transported into the cell where they cause cell damage and eventually cell death. In addition, it seems that the interactions between the membrane interacting ILs, $[P_{4441}][OAc]$ and [Ch][Hex], were too weak to be detected with this technique — the diffusion constants did not change remarkably, indicating that the ILs did not permeate at all or permeated through the plasma membrane without changing the IL diffusion rates significantly. The diffusion constants of the neat membrane disrupting ILs $[P_{14444}][OAc]$ and $[P_{14444}]Cl$, on the other hand, decreased upon increasing concentration of ILs due to aggregation as shown in Figure 16.

The most abrupt decrease in the slope was seen at 520–550 $mg \cdot L^{-1}$ of the ILs, indicating the appearance of the first CMC (CMC_1). These changes correlate well with the known CMCs for the ILs (Papers I and II). The continuing decrease of the diffusion coefficients suggests that the ILs keep aggregating to larger undefined shapes. However, a clear CMC_2 could not be determined. Above the

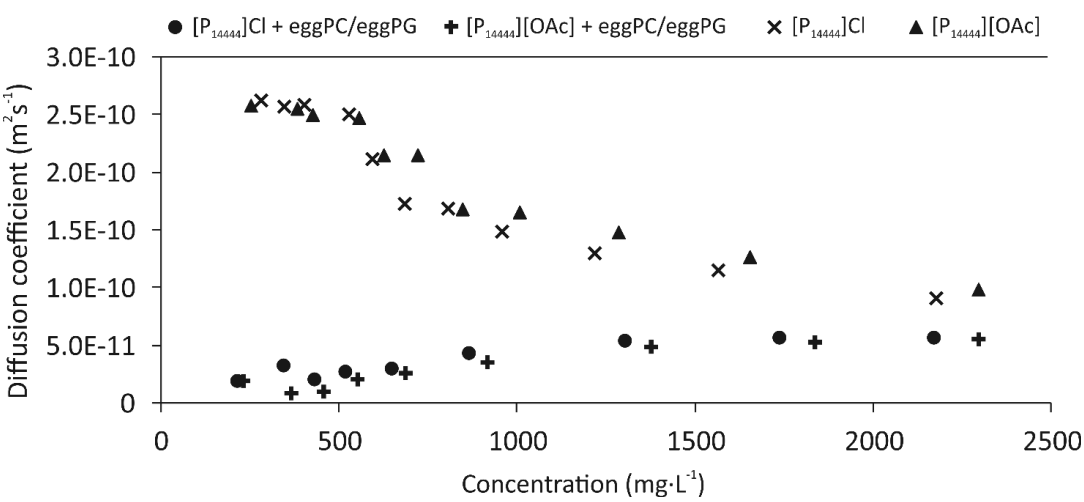

Figure 16. Diffusion coefficients of $[P_{14444}][OAc]$ and $[P_{14444}]Cl$ with and without eggPC/eggPG (80/20 mol%) liposomes. Adapted with permission from "Ruokonen, S.-K., *et al.,* 2018, *Chem.-Eur. J.,* 2018, 24, (11), 2669–2680." Copyright (2018) John Wiley & Sons, Inc.

CMC_1 (520–920 mM), the sizes of the IL aggregates were calculated to be 2.1 nm using the Stokes-Einstein equation (Equation 7). Above 920 mM the sizes increased to 3.5–3.8 nm, evidencing the formation of bigger aggregates.

The size of pure eggPC/eggPG liposomes was calculated to be approximately 120 nm, which correlates well with the DLS data. The diffusion coefficients of the ILs decreased over eight times in the presence of the liposomes, evidencing strong interaction between the ILs and the liposomes. The ILs were shown to disrupt the liposomes at 430–460 $mg \cdot L^{-1}$ (1 mM) concentration, which is shown in the figure as an increase of the diffusion coefficient above 500 $mg \cdot L^{-1}$. At this concentration it is plausible that the ILs behave as common surfactants, as shown before,[13] and saturate the vesicle (saturation point). Upon increasing the concentration above 500 $mg \cdot L^{-1}$, the vesicles start to disrupt and mixed vesicles and mixed micelles coexist until a solvation concentration is reached. At this point there is no vesicles left in the solution. However, the diffusion coefficients do not reach the diffusion coefficients of the neat ILs, indicating a balance between the lipid-IL mixed micelles and the neat IL micelles.

6. CONCLUSIONS

The aim of this doctoral work was to assess the toxicity of ionic liquids using zebrafish, various cell lines, and biomimicking liposomes. First, information on properties that affect the ionic liquid toxicity was collected using zebrafish and various cell lines. Phosphonium-based ionic liquids with long alkyl chains in the cation moiety ($[P_{14444}][OAc]$, $[P_{8444}][OAc]$) were the most toxic ionic liquids tested, causing mortality of cells and malformations of zebrafish. Elongation of the cation moiety instead of the anion moiety by the same carbon amount increased the IL toxicity 70 fold, confirming the cation moiety as the major factor affecting the IL toxicity. This indicates that the total hydrophobicity of the ionic liquid can be increased, without remarkably increasing the toxicity, by elongating the anion instead of the cation. In addition, it was shown that elongation of the IL anion increased the toxicity linearly only when the longest alkyl chain exceeded six carbons. Most of the ILs interacted with the plasma membranes as unimers instead of in the form of aggregates. When the carbon number in the anion reached 16 carbons the cut-off-effect was met and the ILs precipitated, which decreased the IL toxicity. This indicates that IL aggregation and/or precipitation can lower the toxicity of the long alkyl chained anionic ILs.

Furthermore, the toxicity of the ILs is dependent on the tested organism. Bacterial cells were less resistant against the ILs than the mammalian cells. This can be due to a different cell structure or a different detection method. Whereas the toxicity is measured by detecting the decay of bioluminescence of the bacterial cells, the mortality of the mammalian cells is measured.

The time of IL exposure had a significant impact on the IL toxicity. Surface-active ILs could induce toxicity within minutes whereas the non-surface-active ILs, which affected the metabolism of the test organisms, induced mortality after several hours. Also ILs, exerting toxicity both by affecting the metabolism and the plasma membrane, did not cause any membrane damage even at concentrations multiple times above their EC_{50} values if the exposure time was too short (IL exposure time < time causing cell damage at the EC_{50} concentration).

Liposomes, comprising phosphatidylcholine and phosphatidylglycerol and no cholesterol were the preeminent option for the IL-plasma membrane interaction studies. Dynamic light scattering was utilized for attaining information on the IL concentration inducing liposome rupturing. Zeta potential measurements were used for detecting the concentration where the IL is permanently sorbed into the liposome, converting the liposome surface charge. In addition, if the IL-liposome interaction is weak the liposome charge is neutralized, not converted. Differential scanning calorimetry results, on the other hand, revealed the EC_{50} concentration ranges for surface-active ILs. PFG NMR was used for studying the aggregation of ILs and IL-lipid aggregates. It also revealed whether the surface-active IL unimers are fully bound to liposomes or if they occurred as free unimers in the solution.

The analytical methodologies presented in this thesis provided methods for assessing the toxicity of ILs inducing toxicity through IL-plasma membrane interactions, without the use of living organisms. Based on the results from the analytical methodologies the ILs were divided into three categories: 1) liposome rupturing ILs ($[P_{14444}][OAc]$, $[P_{14444}]Cl$, and $[P_{4441}][OAc]$) 2) ILs affecting the metabolism as well as plasma membranes ($[N_{4441}][OAc]$, and [Ch][Hex]), and 3) ILs having an effect solely on the cell metabolism ([emim][OAc], [Ch][OAc], and [DBNH][OAc).

Based on the results of this study it is likely that surface-active ILs exert toxicity by intercalating the cell membrane. However, it is more difficult to predict the mechanism of toxicity of moderately surface-active ILs. The easiest way to determine whether the IL permeates into the membrane or if it is adsorbed onto the membrane is to use differential scanning calorimetry. However, if the IL exerts toxicity also metabolically other methodologies need to be used as well. For example, determining the EC_{50} values using two different dyes, which highlight different mechanism of toxicities, on a cell line is recommended. Also, if ILs with hydrophobic properties want to be used in an application, it is recommended to elongate the anion moiety instead of the cation moiety, in order to avoid remarkable increase of the toxicity.

7. REFERENCES

1. Rogers, R. D.; Seddon, K. R., *Ionic liquids: industrial applications for green chemistry*. ACS Publications: Washington, DC, 2002.
2. Rogers, R. D.; Seddon, K. R.; Volkov, S., *Green industrial applications of ionic liquids*. Springer-Science+Business Media, B.V.: 2002.
3. Machatha, S. G.; Yalkowsky, S. H. Comparison of the octanol/water partition coefficients calculated by ClogP®, ACDlogP and KowWin® to experimentally determined values. *Int. J. Pharm.* **2005,** *294*, (1), 185-192.
4. Cvjetko Bubalo, M.; Radošević, K.; Radojčić Redovniković, I.; Halambek, J.; Gaurina Srček, V. A brief overview of the potential environmental hazards of ionic liquids. *Ecotox. Environ. Safe.* **2014,** *99*, 1-12.
5. Thuy Pham, T. P.; Cho, C.-W.; Yun, Y.-S. Environmental fate and toxicity of ionic liquids: a review. *Water Res.* **2010,** *44*, (2), 352-372.
6. GUIDELINE, D. U. T. OECD Guidelines for the Testing of Chemicals. In OECD, OECD Publishing, Paris, France: 2001.
7. Andersen, M. E.; Krewski, D. Toxicity testing in the 21st century: bringing the vision to life. *Toxicol. Sci.* **2008,** *107*, (2), 324-330.
8. Alberts, B.; Johnson, A.; Lewis, J.; Raff, M.; Roberts, K.; Walter, P., *Molecular biology of the cell*. 5th ed.; Garland Science: New York NY 10016, USA 2008.
9. Burcham, P. C., *An introduction to toxicology*. Springer: 2013.
10. Kontro, I.; Svedström, K.; Duša, F.; Ahvenainen, P.; Ruokonen, S.-K.; Witos, J.; Wiedmer, S. K. Effects of phosphonium-based ionic liquids on phospholipid membranes studied by small-angle X-ray scattering. *Chem. Phys. Lipids* **2016,** *201*, 59-66.
11. Gal, N.; Malferarri, D.; Kolusheva, S.; Galletti, P.; Tagliavini, E.; Jelinek, R. Membrane interactions of ionic liquids: possible determinants for biological activity and toxicity. *Biochim. Biophys. Acta-Biomembr.* **2012,** *1818*, (12), 2967–2974.
12. Ranke, J.; Muller, A.; Bottin-Weber, U.; Stock, F.; Stolte, S.; Arning, J.; Stormann, R.; Jastorff, B. Lipophilicity parameters for ionic liquid cations and their correlation to in vitro cytotoxicity. *Ecotox. Environ. Safe.* **2007,** *67*, (3), 430-438.
13. Jing, B.; Lan, N.; Qiu, J.; Zhu, Y. Interaction of Ionic Liquids with Lipid Bilayer: A Biophysical Study of Ionic Liquid Cytotoxicity. *J. Phys. Chem. B* **2016,** *120*, (10), 2781-2789.
14. Galluzzi, M.; Zhang, S. W.; Mohamadi, S.; Vakurov, A.; Podesta, A.; Nelson, A. Interaction of Imidazolium-Based Room-Temperature Ionic Liquids with DOPC Phospholipid Monolayers: Electrochemical Study. *Langmuir* **2013,** *29*, (22), 6573-6581.
15. Ranke, J.; Cox, M.; Müller, A.; Schmidt, C.; Beyersmann, D. Sorption, cellular distribution, and cytotoxicity of imidazolium ionic liquids in mammalian cells–influence of lipophilicity. *Toxicol Environ. Chem.* **2006,** *88*, (2), 273-285.
16. Galletti, P.; Malferrari, D.; Samori, C.; Sartor, G.; Tagliavini, E. Effects of ionic liquids on membrane fusion and lipid aggregation of egg-PC liposomes. *Colloid Surf. B-Biointerfaces* **2015,** *125*, 142-150.
17. Evans, K. O. Room-temperature ionic liquid cations act as short-chain surfactants and disintegrate a phospholipid bilayer. *Colloid Surf. A-Physicochem. Eng. Asp.* **2006,** *274*, (1), 11-17.
18. Matzke, M.; Arning, J.; Ranke, J.; Jastorff, B.; Stolte, S., Design of inherently safer ionic liquids: toxicology and biodegradation. In *Handbook of Green Chemistry*, Bremen, Germany, 2010; pp 233–298.
19. Walden, P. Molecular weights and electrical conductivity of several fused salts. *Bull. Acad. Imper. Sci.(St. Petersburg)* **1914,** *1800*.
20. Plechkova, N. V.; Seddon, K. R. Applications of ionic liquids in the chemical industry. *Chem. Soc. Rev.* **2008,** *37*, (1), 123-150.
21. Heckenbach, M. E.; Romero, F. N.; Green, M. D.; Halden, R. U. Meta-analysis of ionic liquid literature and toxicology. *Chemosphere* **2016,** *150*, 266-274.

22. Barrer, R. The viscosity of pure liquids. II. Polymerised ionic melts. *Trans. Faraday Soc.* **1943,** *39*, 59-67.
23. Heymann, E.; Bloom, H. Activation Energy of Ionic Migration in Molten Salts. *Nature* **1945,** *156*, 479-480.
24. Harrap, B.; Heymann, E. Theories of viscosity applied to ionic liquids. *Chem. Rev.* **1951,** *48*, (1), 45-67.
25. Elton, G. In *Electroviscosity. III. Sedimentation phenomena in ionic liquids*, Proceedings of the Royal Society of London A: Mathematical, Physical and Engineering Sciences, 1949; The Royal Society: 1949; pp 568-572.
26. Marsh, K.; Boxall, J.; Lichtenthaler, R. Room temperature ionic liquids and their mixtures—a review. *Fluid Phase Equilib.* **2004,** *219*, (1), 93-98.
27. Amde, M.; Liu, J.-F.; Pang, L. Environmental Application, Fate, Effects, and Concerns of Ionic Liquids: A Review. *Environ. Sci. Technol.* **2015,** *49*, (21), 12611-12627.
28. Egorova, K. S.; Gordeev, E. G.; Ananikov, V. P. Biological activity of ionic liquids and their application in pharmaceutics and medicine. *Chem. Rev.* **2017,** *117*, (10), 7132-7189.
29. BASF. http://www.intermediates.basf.com/chemicals/ionic-liquids/index (19.12.2017),
30. IoLiTech https://iolitec.de/en (19.12.2017),
31. Wasserscheid, P.; Welton, T., *Ionic liquids in synthesis*. John Wiley & Sons: 2008.
32. Qureshi, Z. S.; Deshmukh, K. M.; Bhanage, B. M. Applications of ionic liquids in organic synthesis and catalysis. *Clean Technol. Environ. Policy* **2014,** *16*, (8), 1487-1513.
33. Sun, P.; Armstrong, D. W. Ionic liquids in analytical chemistry. *Anal. Chim. Acta* **2010,** *661*, (1), 1-16.
34. Toledo Hijo, A. A.; Maximo, G. J.; Costa, M. C.; Batista, E. A.; Meirelles, A. J. Applications of Ionic Liquids in the Food and Bioproducts Industries. *ACS Sustain. Chem. Eng.* **2016,** *4*, (10), 5347-5369.
35. Holding, A. J.; Heikkilä, M.; Kilpeläinen, I.; King, A. W. T. Amphiphilic and phase-separable ionic liquids for biomass processing. *ChemSusChem* **2014,** *7*, (5), 1422-1434.
36. Muhammad, N.; Man, Z.; Khalil, M. A. B. Ionic liquid—a future solvent for the enhanced uses of wood biomass. *Eur. J. Wood Wood Prod.* **2012,** *70*, (1-3), 125-133.
37. Tsunashima, K.; Sugiya, M. Physical and electrochemical properties of low-viscosity phosphonium ionic liquids as potential electrolytes. *Electrochem. Commun.* **2007,** *9*, (9), 2353-2358.
38. Deetlefs, M.; Seddon, K. R. Assessing the greenness of some typical laboratory ionic liquid preparations. *Green Chem.* **2010,** *12*, (1), 17-30.
39. Anastas, P. T.; Kirchhoff, M. M. Origins, current status, and future challenges of green chemistry. *Accounts Chem. Res.* **2002,** *35*, (9), 686-694.
40. Hwang, J.-h.; Park, H.; Choi, D. W.; Nam, K. T.; Lim, K.-M. Investigation of dermal toxicity of ionic liquids in monolayer-cultured skin cells and 3D reconstructed human skin models. *Toxicol. Vitro* **2018,** *46*, 194-202.
41. Egorova, K. S.; Ananikov, V. P. Toxicity of ionic liquids: eco(cyto) activity as complicated, but unavoidable parameter for task-specific optimization. *ChemSusChem* **2014,** *7*, (2), 336-360.
42. Costa, S. P.; Azevedo, A. M.; Pinto, P. C.; Saraiva, M. Environmental Impact of Ionic Liquids: Recent Advances in (Eco) toxicology and (Bio) degradability. *ChemSusChem* **2017,** *10*, (11), 2321-2347.
43. Reid, J. E.; Prydderch, H.; Spulak, M.; Shimizu, S.; Walker, A. J.; Gathergood, N. Green profiling of aprotic versus protic ionic liquids: Synthesis and microbial toxicity of analogous structures. *Sust. Chem. Pharm.* **2018,** *7*, 17-26.
44. Li, A. P. In vitro approaches to evaluate ADMET drug properties. *Curr. Top. Med. Chem.* **2004,** *4*, (7), 701-706.
45. Liebler, D. C.; Guengerich, F. P. Elucidating mechanisms of drug-induced toxicity. *Nat. Rev. Drug Discov.* **2005,** *4*, (5), 410-420.
46. Jastorff, B.; Störmann, R.; Ranke, J.; Mölter, K.; Stock, F.; Oberheitmann, B.; Hoffmann, W.; Hoffmann, J.; Nüchter, M.; Ondruschka, B. How hazardous are ionic liquids? Structure–activity relationships and biological testing as important elements for sustainability evaluation. *Green Chem.* **2003,** *5*, (2), 136-142.

47. Lichtenberg, D.; Ahyayauch, H.; Alonso, A.; Goni, F. M. Detergent solubilization of lipid bilayers: a balance of driving forces. *Trends Biochem. Sci.* **2013,** *38*, (2), 85-93.
48. Yoo, B.; Shah, J. K.; Zhu, Y.; Maginn, E. J. Amphiphilic interactions of ionic liquids with lipid biomembranes: a molecular simulation study. *Soft Matter* **2014**, 8641-8651.
49. Heerklotz, H. Interactions of surfactants with lipid membranes. *Q. Rev. Biophys.* **2008,** *41*, (3-4), 205-264.
50. Lopez, O.; de la Maza, A.; Coderch, L.; Lopez-Iglesias, C.; Wehrli, E.; Parra, J. L. Direct formation of mixed micelles in the solubilization of phospholipid liposomes by Triton X-100. *FEBS Lett.* **1998,** *426*, (3), 314-318.
51. Hayakawa, E. H.; Mochizuki, E.; Tsuda, T.; Akiyoshi, K.; Matsuoka, H.; Kuwabata, S. The effect of hydrophilic ionic liquids 1-ethyl-3-methylimidazolium lactate and choline lactate on lipid vesicle fusion. *Plos One* **2013,** *8*, (12), e85467.
52. LoPachin, R. M.; Gavin, T.; DeCaprio, A.; Barber, D. S. Application of the hard and soft, acids and bases (HSAB) theory to toxicant–target interactions. *Chem. Res. Toxicol.* **2011,** *25*, (2), 239-251.
53. Fan, Y.; Dong, X.; Yan, L.; Li, D.; Hua, S.; Hu, C.; Pan, C. Evaluation of the toxicity of ionic liquids on trypsin: A mechanism study. *Chemosphere* **2016,** *148*, (Supplement C), 241-247.
54. Stock, F.; Hoffmann, J.; Ranke, J.; Störmann, R.; Ondruschka, B.; Jastorff, B. Effects of ionic liquids on the acetylcholinesterase–a structure–activity relationship consideration. *Green Chem.* **2004,** *6*, (6), 286-290.
55. Składanowski, A.; Stepnowski, P.; Kleszczyński, K.; Dmochowska, B. AMP deaminase in vitro inhibition by xenobiotics: A potential molecular method for risk assessment of synthetic nitro-and polycyclic musks, imidazolium ionic liquids and N-glucopyranosyl ammonium salts. *Environ. Toxicol. Pharmacol.* **2005,** *19*, (2), 291-296.
56. Westerfield, M., *The zebrafish book: a guide for the laboratory use of zebrafish (Danio rerio)*. University of Oregon Press: 2000.
57. Hill, A. J.; Teraoka, H.; Heideman, W.; Peterson, R. E. Zebrafish as a model vertebrate for investigating chemical toxicity. *Toxicol. Sci.* **2005,** *86*, (1), 6-19.
58. Omasa, T.; Onitsuka, M.; Kim, W.-D. Cell engineering and cultivation of Chinese hamster ovary (CHO) cells. *Curr. Pharm. Biotechnol.* **2010,** *11*, (3), 233-240.
59. Rönkkö, S.; Vellonen, K.-S.; Järvinen, K.; Toropainen, E.; Urtti, A. Human corneal cell culture models for drug toxicity studies. *Drug Deliv. Transl. Res.* **2016,** *6*, (6), 660-675.
60. Kudryasheva, N. S. Bioluminescence and exogenous compounds: Physico-chemical basis for bioluminescent assay. *J. Photochem. Photobiol. B-Biol.* **2006,** *83*, (1), 77-86.
61. Ventura, S. P.; e Silva, F. A.; Gonçalves, A. M.; Pereira, J. L.; Gonçalves, F.; Coutinho, J. A. Ecotoxicity analysis of cholinium-based ionic liquids to Vibrio fischeri marine bacteria. *Ecotox. Environ. Safe.* **2014,** *102*, 48-54.
62. Ventura, S. P.; Marques, C. S.; Rosatella, A. A.; Afonso, C. A.; Goncalves, F.; Coutinho, J. A. Toxicity assessment of various ionic liquid families towards *Vibrio fischeri* marine bacteria. *Ecotox. Environ. Safe.* **2012,** *76*, 162-168.
63. Stolte, S.; Matzke, M.; Arning, J.; Böschen, A.; Pitner, W.-R.; Welz-Biermann, U.; Jastorff, B.; Ranke, J. Effects of different head groups and functionalised side chains on the aquatic toxicity of ionic liquids. *Green Chem.* **2007,** *9*, (11), 1170-1179.
64. Costa, S. P.; Pinto, P. C.; Lapa, R. A.; Saraiva, M. L. M. Toxicity assessment of ionic liquids with Vibrio fischeri: An alternative fully automated methodology. *J. Hazard. Mater.* **2015,** *284*, 136-142.
65. Hernández-Fernández, F. J.; Bayo, J.; Pérez de los Ríos, A.; Vicente, M. A.; Bernal, F. J.; Quesada-Medina, J. Discovering less toxic ionic liquids by using the Microtox® toxicity test. *Ecotox. Environ. Safe.* **2015,** *116*, 29-33.
66. Kokkali, V.; van Delft, W. Overview of commercially available bioassays for assessing chemical toxicity in aqueous samples. *Trac-Trends Anal. Chem.* **2014,** *61*, 133-155.
67. Liu, D.; Dutka, B. J., *Toxicity screening procedures using bacterial systems*. CRC Press: 1984.
68. Docherty, K. M.; Kulpa, C. F. Toxicity and antimicrobial activity of imidazolium and pyridinium ionic liquids. *Green Chem.* **2005,** *7*, (4), 185-189.

69. Lee, S.-M.; Chang, W.-J.; Choi, A.-R.; Koo, Y.-M. Influence of ionic liquids on the growth of Escherichia coli. *Korean J. Chem. Eng.* **2005,** *22*, (5), 687-690.
70. Ganske, F.; Bornscheuer, U. T. Growth of Escherichia coli, Pichia pastoris and Bacillus cereus in the presence of the ionic liquids [BMIM][BF4] and [BMIM][PF6] and organic solvents. *Biotechnol. Lett.* **2006,** *28*, (7), 465-469.
71. Jesorka, A.; Orwar, O. Liposomes: technologies and analytical applications. *Annu. Rev. Anal. Chem.* **2008,** *1*, 801-832.
72. Franzen, U.; Østergaard, J. Physico-chemical characterization of liposomes and drug substance–liposome interactions in pharmaceutics using capillary electrophoresis and electrokinetic chromatography. *J. Chromatogr. A* **2012,** *1267*, 32-44.
73. Edwards, K. A., *Liposomes in Analytical Methodologies*. CRC Press: 2016.
74. Gunstone, F. D.; Harwood, J. L.; Padley, F. B., *The Lipid Handbook*. Second Edition ed.; Chapman & Hall London, UK, 1994.
75. Lingwood, D.; Simons, K. Lipid Rafts As a Membrane-Organizing Principle. *Science* **2010,** *327*, (5961), 46-50.
76. Simons, K.; Ikonen, E. How cells handle cholesterol. *Science* **2000,** *290*, (5497), 1721-1726.
77. Simons, K.; Vaz, W. L. Model systems, lipid rafts, and cell membranes 1. *Annu. Rev. Biophys. Biomol. Struct.* **2004,** *33*, 269-295.
78. McMullen, T. P.; Lewis, R. N.; McElhaney, R. N. Cholesterol–phospholipid interactions, the liquid-ordered phase and lipid rafts in model and biological membranes. *Curr. Opin. Colloid Interface Sci.* **2004,** *8*, (6), 459-468.
79. Harder, T.; Simons, K. Caveolae, DIGs, and the dynamics of sphingolipid—cholesterol microdomains. *Curr. Opin. Cell Biol.* **1997,** *9*, (4), 534-542.
80. Mouritsen, O. G.; Zuckermann, M. J. What's so special about cholesterol? *Lipids* **2004,** *39*, (11), 1101-1113.
81. Phillips, J. The energetics of micelle formation. *Trans. Faraday Soc.* **1955,** *51*, 561-569.
82. Pérez-Rodríguez, M.; Prieto, G.; Rega, C.; Varela, L. M.; Sarmiento, F.; Mosquera, V. A comparative study of the determination of the critical micelle concentration by conductivity and dielectric constant measurements. *Langmuir* **1998,** *14*, (16), 4422-4426.
83. Mukerjee, P. The nature of the association equilibria and hydrophobic bonding in aqueous solutions of association colloids. *Adv. Colloid Interfac.* **1967,** *1*, (3), 242-275.
84. Javadian, S.; Kakemam, J. Intermicellar interaction in surfactant solutions; a review study. *J. Mol. Liq.* **2017,** *242*, 115-128.
85. Israelachvili, J. N., 19 - Thermodynamic Principles of Self-Assembly. In *Intermolecular and Surface Forces (Third Edition)*, Academic Press: San Diego, 2011; pp 503-534.
86. Luczak, J.; Hupka, J.; Thoming, J.; Jungnickel, C. Self-organization of imidazolium ionic liquids in aqueous solution. *Colloid Surf. A-Physicochem. Eng. Asp.* **2008,** *329*, (3), 125-133.
87. Charrier, T.; Durand, M. J.; Affi, M.; Jouanneau, S.; Gezekel, H.; Thouand, G., Bacterial bioluminescent biosensor characterisation for on-line monitoring of heavy metals pollutions in waste water treatment plant effluents. In *Biosensors*, InTech: 2010.
88. Miyashiro, T.; Ruby, E. G. Shedding light on bioluminescence regulation in Vibrio fischeri. *Mol. Microbiol.* **2012,** *84*, (5), 795-806.
89. Tu, S. C.; Mager, H. I. Biochemistry of bacterial bioluminescence. *Photochem. Photobiol.* **1995,** *62*, (4), 615-624.
90. Tagliaro, F.; Manetto, G.; Crivellente, F.; Smith, F. A brief introduction to capillary electrophoresis. *Forensic Sci. Int.* **1998,** *92*, (2), 75-88.
91. Gonzalez-Curbelo, M. A.; Varela-Martinez, D. A.; Socas-Rodriguez, B.; Hernandez-Borges, J. Recent applications of nanomaterials in capillary electrophoresis. *Electrophoresis* **2017,** *38*, (19), 2431-2446.
92. Palmer, C. P. Recent progress in the use of ionic polymers as pseudostationary phases for electrokinetic chromatography. *Electrophoresis* **2009,** *30*, (1), 163-168.
93. Wiedmer, S. K.; Lokajová, J. Capillary electromigration techniques for studying interactions between analytes and lipid dispersions. *J. Sep. Sci.* **2013,** *36*, (1), 37-51.
94. Wiedmer, S. K.; Shimmo, R. Liposomes in capillary electromigration techniques. *Electrophoresis* **2009,** *30*, (S1), S240-S257.

95. Wiedmer, S. K.; Lokajová, J.; Riekkola, M. L. Marker compounds for the determination of retention factors in EKC. *J. Sep. Sci.* **2010,** *33*, (3), 394-409.
96. Owen, R. L.; Strasters, J. K.; Breyer, E. D. Lipid vesicles in capillary electrophoretic techniques: Characterization of structural properties and associated membrane-molecule interactions. *Electrophoresis* **2005,** *26*, (4-5), 735-751.
97. Bhattacharjee, S. DLS and zeta potential–What they are and what they are not? *J. Control. Release* **2016,** *235*, 337-351.
98. Worldwide, M. I. Technical note: Dynamic Light Scattering: An Introduction in 30 Minutes. https://warwick.ac.uk/fac/cross_fac/sciencecity/programmes/internal/themes/am2/booking/particlesize/intro_to_dls.pdf
99. Hunter, R. J., *Zeta potential in colloid science: principles and applications*. Academic press: 1981.
100. Worldwide, M. I. Technical note: Zeta potential - An introduction in 30 minutes. http://www.materials-talks.com/wp-content/uploads/2017/09/mrk654-01_an_introduction_to_zeta_potential_v3.pdf
101. Chiu, M. H.; Prenner, E. J. Differential scanning calorimetry: an invaluable tool for a detailed thermodynamic characterization of macromolecules and their interactions. *J. Pharm. Bioallied Sci.* **2011,** *3*, (1), 39.
102. Heerklotz, H. The microcalorimetry of lipid membranes. *J. Phys.-Condens. Matter* **2004,** *16*, (15), R441-R467.
103. Ibarra-Molero, B.; Sanchez-Ruiz, J. M., Differential scanning calorimetry of proteins: an overview and some recent developments. In *Advanced Techniques in Biophysics*, Springer-Verlag: Berlin, Heidelberg, 2006; Vol. 10, pp 27-48.
104. Tariq, M.; Freire, M. G.; Saramago, B.; Coutinho, J. A.; Lopes, J. N. C.; Rebelo, L. P. N. Surface tension of ionic liquids and ionic liquid solutions. *Chem. Soc. Rev.* **2012,** *41*, (2), 829-868.
105. Macomber, R. S., *A complete introduction to modern NMR spectroscopy*. Wiley New York: 1998.
106. Pages, G.; Gilard, V.; Martino, R.; Malet-Martino, M. Pulsed-field gradient nuclear magnetic resonance measurements (PFG NMR) for diffusion ordered spectroscopy (DOSY) mapping. *Analyst* **2017,** *142*, (20), 3771-3796.
107. Parviainen, A.; King, A. W. T.; Mutikainen, I.; Hummel, M.; Selg, C.; Hauru, L. K. J.; Sixta, H.; Kilpeläinen, I. Predicting Cellulose Solvating Capabilities of Acid–Base Conjugate Ionic Liquids. *ChemSusChem* **2013,** *6*, (11), 2161-2169.
108. King, A. W.; Parviainen, A.; Karhunen, P.; Matikainen, J.; Hauru, L. K.; Sixta, H.; Kilpeläinen, I. Relative and inherent reactivities of imidazolium-based ionic liquids: the implications for lignocellulose processing applications. *RSC Advances* **2012,** *2*, (21), 8020-8026.
109. Bligh, E. G.; Dyer, W. J. A rapid method of total lipid extraction and purification. *Can. J. Biochem. Phys.* **1959,** *37*, (8), 911-917.
110. Reer, O.; Bock, T. K.; Müller, B. W. In vitro corneal permeability of diclofenac sodium in formulations containing cyclodextrins compared to the commercial product voltaren ophtha. *J. Pharm. Sci.* **1994,** *83*, (9), 1345-1349.
111. Araki-Sasaki, K.; Ohashi, Y.; Sasabe, T.; Hayashi, K.; Watanabe, H.; Tano, Y.; Handa, H. An SV40-immortalized human corneal epithelial cell line and its characterization. *Invest. Ophthalmol. Vis. Sci.* **1995,** *36*, (3), 614-621.
112. Secretariat, U. N. E. C. f. E. *Globally Harmonized System of Classification and Labelling of Chemicals (GHS)*; United Nations Publications 2003.
113. Larson, E. M.; Doughman, D. J.; Gregerson, D. S.; Obritsch, W. F. A new, simple, nonradioactive, nontoxic in vitro assay to monitor corneal endothelial cell viability. *Invest. Ophthalmol. Vis. Sci.* **1997,** *38*, (10), 1929-1933.
114. ThermoFischer Scientific - alamarBlue® Cell Viability Assay Protocol. https://www.thermofisher.com/fi/en/home/references/protocols/cell-and-tissue-analysis/cell-profilteration-assay-protocols/cell-viability-with-alamarblue.html#4 (9.1.2018),

115. Promega Corporation - Technical Manual: CellTox™ Green Cytotoxicity Assay. https://fi.promega.com/products/cell-health-assays/cell-viability-and-cytotoxicity-assays/celltox-green-cytotoxicity-assay/?catNum=G8741 (6.2.2018),
116. Schullery, S.; Schmidt, C.; Felgner, P.; Tillack, T.; Thompson, T. Fusion of dipalmitoylphosphatidylcholine vesicles. *Biochemistry* **1980,** *19*, (17), 3919-3923.
117. Berry, J. D.; Neeson, M. J.; Dagastine, R. R.; Chan, D. Y.; Tabor, R. F. Measurement of surface and interfacial tension using pendant drop tensiometry. *J. Colloid Interface Sci.* **2015,** *454*, 226-237.
118. Biltonen, R. L.; Lichtenberg, D. The use of differential scanning calorimetry as a tool to characterize liposome preparations. *Chem. Phys. Lipids* **1993,** *64*, (1-3), 129-142.
119. Parab, S.; Bhalerao, S. Choosing statistical test. *Int. J. Ayurveda Res.* **2010,** *1*, (3), 187.
120. Demšar, J. Statistical Comparisons of Classifiers over Multiple Data Sets. *J. Mach. Learn. Res.* **2006,** *7*, 1-30.
121. Kimmel, C. B.; Ballard, W. W.; Kimmel, S. R.; Ullmann, B.; Schilling, T. F. Stages of Embryonic-Development of the Zebrafish. *Dev. Dyn.* **1995,** *203*, (3), 253-310.
122. Sih, A.; Bell, A.; Johnson, J. C. Behavioral syndromes: an ecological and evolutionary overview. *Trends Ecol. Evol.* **2004,** *19*, (7), 372-378.
123. Lachance, B.; Robidoux, P. Y.; Hawari, J.; Ampleman, G.; Thiboutot, S.; Sunahara, G. I. Cytotoxic and genotoxic effects of energetic compounds on bacterial and mammalian cells in vitro. *Mutat. Res. Genet. Toxicol. Environ. Mutagen.* **1999,** *444*, (1), 25-39.
124. Hodgson, E., *A textbook of modern toxicology*. John Wiley & Sons: 2004.
125. Mester, P.; Wagner, M.; Rossmanith, P. Antimicrobial effects of short chained imidazolium-based ionic liquids—Influence of anion chaotropicity. *Ecotox. Environ. Safe.* **2015,** *111*, 96-101.
126. Kulacki, K. J.; Lamberti, G. A. Toxicity of imidazolium ionic liquids to freshwater algae. *Green Chem.* **2008,** *10*, (1), 104-110.
127. Chen, H. L.; Kao, H. F.; Wang, J. Y.; Wei, G. T. Cytotoxicity of imidazole ionic liquids in human lung carcinoma A549 cell line. *J. Chin. Chem. Soc.* **2014,** *61*, (7), 763-769.
128. Bernot, R. J.; Brueseke, M. A.; Evans-White, M. A.; Lamberti, G. A. Acute and chronic toxicity of imidazolium-based ionic liquids on Daphnia magna. *Environ. Toxicol. Chem.* **2005,** *24*, (1), 87-92.
129. Sosnowska, A.; Barycki, M.; Zaborowska, M.; Rybinska, A.; Puzyn, T. Towards designing environmentally safe ionic liquids: the influence of the cation structure. *Green Chem.* **2014,** *16*, (11), 4749-4757.
130. Pernak, J.; Sobaszkiewicz, K.; Mirska, I. Anti-microbial activities of ionic liquids. *Green Chem.* **2003,** *5*, (1), 52-56.
131. Ventura, S. P.; de Barros, R. L.; Sintra, T.; Soares, C. M.; Lima, Á. S.; Coutinho, J. A. Simple screening method to identify toxic/non-toxic ionic liquids: Agar diffusion test adaptation. *Ecotox. Environ. Safe.* **2012,** *83*, 55-62.
132. Petkovic, M.; Ferguson, J. L.; Gunaratne, H. N.; Ferreira, R.; Leitao, M. C.; Seddon, K. R.; Rebelo, L. P. N.; Pereira, C. S. Novel biocompatible cholinium-based ionic liquids—toxicity and biodegradability. *Green Chem.* **2010,** *12*, (4), 643-649.
133. Santos, J. I.; Gonçalves, A. M.; Pereira, J.; Figueiredo, B.; e Silva, F.; Coutinho, J. A.; Ventura, S. P.; Gonçalves, F. Environmental safety of cholinium-based ionic liquids: assessing structure–ecotoxicity relationships. *Green Chem.* **2015,** *17*, (9), 4657-4668.
134. Muhammad, N.; Hossain, M. I.; Man, Z.; El-Harbawi, M.; Bustam, M. A.; Noaman, Y. A.; Alitheen, N. B. M.; Ng, M. K.; Hefter, G.; Yin, C. Y. Synthesis and Physical Properties of Choline Carboxylate Ionic Liquids. *J. Chem. Eng. Data* **2012,** *57*, (8), 2191-2196.
135. Weyhing-Zerrer, N.; Kalb, R.; Oßmer, R.; Rossmanith, P.; Mester, P. Evidence of a reverse side-chain effect of tris (pentafluoroethyl) trifluorophosphate [FAP]-based ionic liquids against pathogenic bacteria. *Ecotox. Environ. Safe.* **2018,** *148*, 467-472.
136. Hartmann, D. O.; Shimizu, K.; Siopa, F.; Leitão, M. C.; Afonso, C. A.; Lopes, J. N. C.; Pereira, C. S. Plasma membrane permeabilisation by ionic liquids: a matter of charge. *Green Chem.* **2015,** *17*, (9), 4587-4598.

137. Liu, H.; Gao, Y.; Hu, Z. Determination of critical micelle concentration values by capillary electrophoresis. *J. Anal. Chem.* **2007,** *62*, (2), 176-178.
138. Cifuentes, A.; Bernal, J. L.; Diez-Masa, J. C. Determination of critical micelle concentration values using capillary electrophoresis instrumentation. *Anal. Chem.* **1997,** *69*, (20), 4271-4274.
139. Mrestani, Y.; Claussen, S.; Neubert, R. H. Determination of CMC of sodium glucocorticides hemisuccinates by CE. *J. Pharm. Biomed. Anal.* **2002,** *30*, (3), 869-873.
140. Swarup, S.; Schoff, C. K. a Survey of Surfactants in Coatings Technology. *Prog. Org. Coat.* **1993,** *23*, (1), 1-22.
141. Chiaraviglio, L.; Kirby, J. E. Evaluation of impermeant, DNA-binding dye fluorescence as a real-time readout of eukaryotic cell toxicity in a high throughput screening format. *Assay Drug Dev. Technol.* **2014,** *12*, (4), 219-228.
142. Gregoriadis, G., *Liposome technology: interactions of liposomes with the biological milieu*. CRC press: 2006; Vol. 3.
143. Naguib, M.; Magboul, M. M.; Samarkandi, A. H.; Attia, M. Adverse effects and drug interactions associated with local and regional anaesthesia. *Drug Saf.* **1998,** *18*, (4), 221-250.
144. Yagiela, J. A. Local anesthetics. *Anesth. prog.* **1991,** *38*, (4-5), 128.
145. Soni, M.; Burdock, G.; Taylor, S.; Greenberg, N. Safety assessment of propyl paraben: a review of the published literature. *Food Chem. Toxicol.* **2001,** *39*, (6), 513-532.
146. Franzen, U.; Ostergaard, J. Physico-chemical characterization of liposomes and drug substance-liposome interactions in pharmaceutics using capillary electrophoresis and electrokinetic chromatography. *J. Chromatogr. A* **2012,** *1267*, 32-44.
147. Ruokonen, S.-K.; Duša, F.; Lokajová, J.; Kilpeläinen, I.; King, A. W.; Wiedmer, S. K. Effect of ionic liquids on the interaction between liposomes and common wastewater pollutants investigated by capillary electrophoresis. *J. Chromatogr. A* **2015,** *1405*, 178-187.
148. Wang, T. T.; Feng, Y.; Jin, X. H.; Fan, X. X.; Crommen, J.; Jiang, Z. J. Liposome electrokinetic chromatography based in vitro model for early screening of the drug-induced phospholipidosis risk. *J. Pharm. Biomed. Anal.* **2014,** *96*, 263-271.
149. Wiedmer, S. K.; Jussila, M. S.; Holopainen, J. M.; Alakoskela, J. M.; Kinnunen, P. K.; Riekkola, M. L. Cholesterol-containing phosphatidylcholine liposomes: characterization and use as dispersed phase in electrokinetic capillary chromatography. *J. Sep. Sci.* **2002,** *25*, (7), 427-437.
150. Muhonen, J.; Holopainen, J. M.; Wiedmer, S. K. Interactions between local anesthetics and lipid dispersions studied with liposome electrokinetic capillary chromatography. *J. Chromatogr. A* **2009,** *1216*, (15), 3392-3397.
151. Rengstl, D.; Kraus, B.; Van Vorst, M.; Elliott, G. D.; Kunz, W. Effect of choline carboxylate ionic liquids on biological membranes. *Colloid Surf. B: Biointerfaces* **2014,** *123*, 575-581.